Pharmacological Research 133 (2018) 35–52

Contents lists available at ScienceDirect

Pharmacological Research

journal homepage: www.elsevier.com/locate/yphrs

Invited Review

The role of small molecule Kit protein-tyrosine kinase inhibitors in the treatment of neoplastic disorders

Robert Roskoski Jr.

Blue Ridge Institute for Medical Research, 3754 Brevard Road, Suite 116, Box 19, Horse Shoe, NC 28742-8814, United States

ARTICLE INFO

Chemical compounds studied in this article:
Axitinib: (PubMED CID: 6450551)
Cabozantinib (PubMED CID: 25102847)
Dasatinib: (PubMED CID: 3062316)
Imatinib: (PubMED CID: 5291)
Lenvatinib: (PubMED CID: 9823820)
Midostaurin: (PubMED CID: 9829523)
Ponatinib: (PubMed CID: 24826799)
Regorafenib: (PubMed CID: 11167602)
Sorafenib: (PubMed CID: 216239)
Sunitinib: (PubMed CID: 5329102)

Keywords:
Catalytic spine
K/E/D/D
Protein kinase inhibitor classification
Protein kinase structure
Targeted cancer therapy

ABSTRACT

The Kit proto-oncogene was found as a consequence of the discovery of the feline *v-kit* sarcoma oncogene. Stem cell factor (SCF) is the Kit ligand and it mediates Kit dimerization and activation. The Kit receptor contains an extracellular segment that is made up of five immunoglobulin-like domains (D1/2/3/4/5), a transmembrane segment, a juxtamembrane segment, a protein-tyrosine kinase domain that contains an insert of 77 amino acid residues, and a carboxyterminal tail. Activating somatic mutations in Kit have been documented in various neoplasms including gastrointestinal stromal tumors (GIST), mast cell overexpression (systemic mastocytosis), core-binding factor acute myeloid leukemias (AML), melanomas, and seminomas. In the case of gastrointestinal stromal tumors, most activating mutations occur in the juxtamembrane segment and these mutants are initially sensitive to imatinib. As with many targeted anticancer drugs, resistance to Kit antagonists occurs in about two years and is the result of secondary *KIT* mutations. An activation segment exon 17 D816V mutation is one of the more common resistance mutations in Kit and this mutant is resistant to imatinib and sorafenib. Type I protein kinase inhibitors interact with the active enzyme form with DFG-D of the proximal activation segment directed inward toward the active site (DFG-D_{in}). In contrast, type II inhibitors bind to their target with the DFG-D pointing away from the active site (DFG-D_{out}). Based upon the X-ray crystallographic structures, imatinib, sunitinib, and ponatinib are Type II Kit inhibitors. We used the Schrödinger induced fit docking protocol to model the interaction of midostaurin with Kit and the result indicates that it binds to the DFG-D_{in} conformation of the receptor and is thus classified as type I inhibitor. This medication inhibits the notoriously resistant Kit D816V mutant and is approved for the treatment of systemic mastocytosis and is effective against tumors bearing the D816V activation/resistance mutation.

1. Functions of the stem cell factor (SCF) ligand and its receptor (Kit)

Protein kinases are enzymes that perform a central role in nearly every aspect of cell biology and biochemistry [1,2]. They form signaling modules that regulate apoptosis, cell cycle progression, proliferation, cytoskeletal rearrangement, differentiation, development, motility, nervous system function, transcription, and translation. Owing to the extensive actions of protein kinases, it is essential that they are stringently regulated because abnormal activity of these enzymes leads to cardiovascular, inflammatory, and nervous disorders along with cancer and diabetes. Because mutations, overexpression, and dysregulation of protein kinases play causal roles in the pathogenesis of human disease, these enzymes represent attractive drug targets [3].

Protein kinases catalyze the following reaction:

$$MgATP^{1-} + protein\text{–}O\text{:}H \rightarrow protein\text{–}O\text{:}PO_3^{2-} + MgADP + H^+$$

Based upon the nature of the phosphorylated −OH group, these protein catalysts are classified as protein-serine/threonine, protein-tyrosine, or dual specificity protein kinases. Manning et al. catalogued 478 typical and 40 atypical protein kinase genes in humans (518 total) along with 106 pseudogenes [4]. The entire family includes 385 protein-serine/threonine kinases, 90 protein-tyrosine kinases, and 43 protein-tyrosine kinase-like enzymes. Of the 90 protein-tyrosine kinases, a total of 32 are cytosolic non-receptor enzymes and 58 are receptors with an extracellular, transmembrane, and intracellular domain. A small group of enzymes, which includes MEK1 and MEK2, are cytosolic dual-specificity kinases that catalyze the phosphorylation of both

Abbreviations: AS, activation segment; CS or C-spine, catalytic spine; CL, catalytic loop; CTT, carboxyterminal tail; D1, immunoglobulin-like domain-1; EGFR, epidermal growth factor receptor; GIST, gastrointestinal stromal tumors; GK, gatekeeper; GRL, Gly-rich loop; KD, kinase domain; KID, kinase insert domain; JM, juxtamembrane; PDGFR, platelet-derived growth factor receptor; PKA, protein kinase A; Ph^+, Philadelphia chromosome positive; PKC, protein kinase C; pY or pTyr, phosphotyrosine; RS or R-spine, regulatory spine; Sh2, shell residue 2; TM, transmembrane; VEGFR, vascular endothelial growth factorreceptor

E-mail address: rrj@brimr.org.

https://doi.org/10.1016/j.phrs.2018.04.020
Received 23 April 2018; Accepted 23 April 2018
Available online 25 April 2018
1043-6618/

threonine and then tyrosine. These enzymes closely resemble and are classified with protein-serine/threonine kinases. Based upon chromosomal mapping, Manning et al. reported that 244 of 518 protein kinase genes are located at disease loci or cancer amplicons (gene amplifications) [4], a result that further emphasizes the importance of protein kinase antagonists as possible drug targets. The protein-phosphatase superfamily of enzymes mediates the dephosphorylation of proteins thereby making phosphorylation-dephosphorylation an overall reversible process [5].

Besmer et al. identified the Hardy-Zuckerman 4 feline retroviral sarcoma oncogene in 1986 and designated the oncogenic transforming factor as *v-kit* [6]. The original sample was obtained from a 7-year-old domestic cat (St. Louis, Missouri USA); thus, the *v-kit* designation does not refer to kitten and is entirely arbitrary. Yarden et al. subsequently cloned the gene and determined the primary structure of Kit, the normal cellular homologue or proto-oncogene corresponding to *v-kit* [7]. They reported that the amino acid sequence of Kit corresponded to a receptor protein-tyrosine kinase based upon its homology with PDGFR and colony-stimulating factor-1 receptor. The Kit ligand was identified in 1990 and variously named (i) Kit ligand, (ii) mast cell growth factor, (iii) Steel factor (where Steel is a mouse mutant) and (iv) stem cell factor (SCF) [8].

In both the developing animal and in adults, stem cells have the ability to balance differentiation and self-renewal such that mature cells essential for the development and function of specific cell types and organs can be produced and replaced without reducing the stem cell pool. Furthermore, Kit and SCF play central roles in cell differentiation, proliferation, and survival. Kit signaling is important in several processes including erythropoiesis, gametogenesis, lymphopoiesis, mast cell development, and melanogenesis [9]. Kit is expressed in (i) hematopoietic stem cells, (ii) dendritic, erythroid, and myeloid progenitor cells, and (iii) pro-B and pro-T cells [10]. The origin of the concept of stem cell factor referred initially to its role in the self-renewal, survival, and differentiation of hematopoietic stem cells. Kit expression is downregulated or lost during cell differentiation with the exceptions of the interstitial cells of Cajal in the gut, mature mast cells, and melanocytes. Moreover, the adult mouse oocyte expresses the Kit receptor while the surrounding granulosa cells express the SCF activating ligand. Defects in Kit function have been reported to produce abnormal peripheral nerve regeneration and spatial learning memory deficits in mice [11,12].

Kit, macrophage/colony stimulating factor-1 receptor or Fms (which refers to feline McDonough sarcoma virus), Flt3 (Fms-like tyrosine kinase-3), PDGFRα, and PDGFRβ are type III receptor protein-tyrosine kinases. See Refs. [13,14] for a description of the 20 types of receptor protein-tyrosine kinases. Each of the type III receptors contains an extracellular segment with five immunoglobulin-like domains (D1–D5), a transmembrane segment, an intracellular domain that consists of a juxtamembrane (JM) segment, a protein kinase domain that contains an insert of several amino acid residues, and a carboxyterminal tail [15]. Two main isoforms of Kit exist based upon the inclusion (^{510} GNNK^{513}) or exclusion (GNNK^{-}) of four residues after D5. The Kit intracellular segment consists of a JM segment, a protein kinase domain that contains an insert of 77 amino acid residues, and a carboxyterminal tail (Fig. 1). The SCF gene product contains 273 residues [8]. After cleavage of its signal sequence (residues 1–25), it consists of an extracellular domain (residues 26–214), a transmembrane segment (215–237), and a short intracellular domain (238–273). SCF expressed with exon 6 in the extracellular domain contains a proteolytic cleavage site that undergoes hydrolysis to release a soluble factor containing 165 amino acid residues (Fig. 1). The proteases that may be responsible for the cleavage of membrane-bound SCF include matrix metalloprotease-9, chymase-1, and members of the ADAM (a disintegrin and metalloproteinase) family [9]. Two protomers combine noncovalently to form a SCF head-to-head dimer. When the gene is expressed lacking exon 6, SCF is able to form an active membrane-bound dimer, each protomer of which contains 220 amino acid residues.

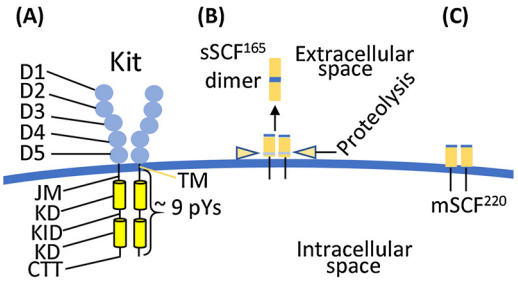

Fig. 1. (A) Overall structure of Kit. (B) Proteolysis at exon 6 liberates the soluble form of SCF, which forms a head-to-head dimer. (C) Membrane-bound SCF. D1, immunoglobulin-like domain 1; TM, transmembrane; JM, juxtamembrane; KD, kinase domain; KID, kinase insert domain; CTT, carboxyterminal tail; pY, phosphotyrosine; mSCF, membrane-bound SCF; sSCF, soluble SCF.

2. *KIT* mutations and human disease

Loss-of-function *KIT* mutations in humans lead to piebaldism, a rare autosomal-dominant disease [16]. This condition is characterized by abnormal pigmentation of the hair and skin, deafness, and megacolon. Furitsu et al. reported the first activating mutations of *KIT* in the HMC-1 human mast cell leukemia cell line [17]. They observed an exon 11 V560G and an exon 17 D816V mutation in the same allele that correspond to the Kit juxtamembrane segment and activation loop, respectively. Gain-of-function somatic mutations occur in a variety of human neoplasms including gastrointestinal stromal tumors (GIST), aggressive systemic mastocytosis, core-binding factor acute myeloid leukemias (AML), melanomas, and seminomas [8,9,18–20]. Note that the location of the various mutations varies among the various types of neoplasms. (Table 1). About 75–80% of cases of GIST bear activating *KIT* mutations [22]. Additionally, point mutations in the *PDGFRA* gene result in the production of an activated PDGFRα that occurs in about 5–7% of these neoplasms [23].

The tumors of patients with GIST originate from the interstitial cells of Cajal and are most commonly found in the stomach (≈60%), jejunum and ileum (≈30%), duodenum (≈5%), colon and rerectum (≈5%), and vary rarely in the esophagus [24,25]. Surgery is the first-line treatment. In patients with recurrent disease or with metastases, treatment with Kit inhibitors including imatinib has been very effective [26]. As noted in Section 3.3, secondary resistance occurs as a result of additional *KIT* mutations and sunitinib and then regorafenib represents second- and third-line treatments. Resistance to first-line imatinib occurs in about two years [27]. In contrast, resistance to second- and third-line sunitinib and regorafenib occurs in about six months [28,29]. Accordingly, the development of new drugs and new approaches in the treatment of advanced GIST is desirable. About 10% of these mutations involve the insertion of AY 502–503 in exon 9, which corresponds to D5 in the extracellular domain. Approximately 67% of the GIST mutations occur in exon 11 and correspond to the juxtamembrane segment. These mutations include deletions in the region of K550–E561 and deletion of D579. The most common exon 11 mutations include V559D and V560D. The K642E exon 13 mutation within the proximal kinase domain occurs rarely in GIST. The number of new cases of GIST diagnosed in the United States is about 5000 per year [30]. For a summary of the clinical trials that led to the approval of imatinib, sunitinib, and regorafenib as well as other drugs in clinical trials for the treatment of GIST, see Refs. [26,31].

Activating *KIT* mutations occur in greater than 90% of all cases of systemic mastocytosis [21]. This disorder is a myeloid neoplasm that is associated with the accumulation of abnormal mast cells in the bone marrow, liver, skin, and spleen. As a consequence, patients suffer from weight loss, ascites, bone lesions, anemia, neutropenia,

Table 1
Location of primary *KIT* activating mutations and secondary resistance mutations.[a]

Domain	Exon	Primary mutation[b]	Diseases[c]
Extracellular domain D5	8	L416	CBF-AML
		T417	CBF-AML
		Y418	CBF-AML
		D419	CBF-AML, GIST, mastocytosis
		A502	GIST
	9	Y503	GIST
		K509	Mastocytosis
Transmembrane segment	10	F522	Mastocytosis
		V530	CBF-AML
		A533	Mastocytosis
Juxtamembrane segment	11	K550	GIST
		P551	GIST
		M552	GIST
		Y553	GIST
		V554*	GIST
		V555	GIST
		Q556	GIST
		W557*	GIST, seminoma
		K558	GIST
		V559*	GIST, mastocytosis
		V560*	GIST, mastocytosis
		E561	GIST
		L576*	Seminoma, melanoma
		D579*	GIST
Kinase domain	13	K642*	GIST
		T670*	Secondary mutation only
Kinase insert domain	14	K704	GIST
		N705	GIST
	15	S715	GIST
Activation segment	17	R815	Mastocytosis
		D816*	CBF-AML, mastocytosis, seminoma
		I817	Mastocytosis
		D820*	Mastocytosis, seminoma
		N822*	CBF-AML, seminoma
		Y823*	Seminoma
	18	A829*	Secondary mutation only
		E839	Mastocytosis

[a] Data from Ref. [21].
[b] Secondary disease resistant mutations are denoted with an asterisk*.
[c] CBF-AML, core-binding factor acute myelogenous leukemia, GIST, gastrointestinal stromal tumors.

thrombocytopenia, and abnormal liver function tests. Following the release of histamine, leukotrienes, prostaglandins, cytokines, and other substances from mast cells, patients experience pruritus (itching), flushing of the skin, and nasal discharge (rhinorrhea). Advanced systemic mastocytosis has a poor prognosis; the median overall survival is 3.5 years in patients with aggressive systemic mastocytosis, 2 years in patients with systemic mastocytosis with an associated hematologic neoplasm (usually a myelodysplastic syndrome, myeloproliferative disorder, or acute myeloid leukemia), and less than 6 months in patients with mast cell leukemia [32]. Cladribine and interferon alpha are associated with major responses in about 50% and 20% of these patients, respectively. Imatinib and midostaurin are protein-tyrosine kinase inhibitors that are approved for the treatment of advanced systemic mastocytosis. Most of the *KIT* mutations (> 90%) are activating D816V/Y/F mutations that occur in exon 17 and are found within the activation segment [21]. A small number of additional mutations including those of exon 10 F522C and A533D and exon 11 V559I and V560G are found in the Kit transmembrane segment. The estimated incidence of this disorder is 5–10 per million people [33], which corresponds to about 1600–3200 cases per year in the United States.

Core-binding factor leukemia, which makes up about 15% of cases of acute myeloid leukemia, has a good overall prognosis following treatment with cytarabine with a complete remission occurring in nearly 90% of patients [34]. This leukemia is associated with two cytogenetic abnormalities: t(8;21)(q22;q22) and inv(16)(p13q22) or t(16:16)(p13;q22); *KIT* mutations occur in about 30% of these patients. Most of the mutations occur in the Kit activation segment and include exon 17 D816H/V/Y and N822K mutations [21]. The incidence of mutant *KIT* core-binding factor leukemia in the United States is about 1000 per year.

Although melanoma accounts for about 2% of all skin cancers, it is responsible for about 80% of skin cancer deaths [35]. In many instances, surgery is curative. Other treatment modalities include radiation, immunotherapy, chemotherapy, and targeted therapies. The V600E mutation in B-Raf is present in about 60% of patients with melanoma and two B-Raf inhibitors including vemurafenib and dabrafenib are effective and FDA approved (www.brimr.org/PKI/PKIs.htm) [36]. As with all protein-kinase inhibitors, acquired resistance is the rule rather than the exception. *KIT* amplifications occur in about 35% of patients with melanoma while the frequency of *KIT* mutations is about 3% [36,37]. The exon 11 L576P JM segment mutation is the most common mutation. Of note, Kit inhibitors are effective in patients with *KIT* mutations, but they are ineffective in patients with *KIT* amplification. The incidence of melanoma is about 90,000 per year [35] so that the number with *KIT* mutations is about 2700.

Seminomas are germ cell tumors with a good prognosis owing to a very low incidence of metastasis and to the effectiveness of traditional cytotoxic therapies. The number of new cases of testicular cancer in the United States is about 9300 per year [35] and most of these are (≈5000) are seminomas. Of the seminomas, perhaps 10–15% possess activating *KIT* mutations [21]. These include the transmembrane segment exon 11 W557C/R and L576P mutations and the activation segment exon 17 D816H/V/Y, N822K, and Y823C/D/N mutations. D816V is the most common seminoma mutation. Thus far treatment of seminomas with activating Kit mutations has been ineffective and treatment with Kit antagonists is not being tested in clinical trials (www.clinicaltrials.gov). Furthermore, autocrine or paracrine activation, but not mutations, of Kit has been hypothesized in other human neoplasms including ovarian and small-cell lung cancers [38]. The incidence of chronic myelogenous leukemia is about 10,000 new cases per year for which imatinib and second- and third-generation BCR-Abl non-receptor protein kinase inhibitors have proven clinically effective and commercially successful [2]. By comparison, the overall incidence of *KIT* mutations in cancer is about 12,000 per year in the United States, but not all of these represent prime Kit targets.

3. Properties of the Kit protein-tyrosine kinase domain

3.1. Primary, secondary, and tertiary structures of the Kit catalytic domain

The catalytic domain of Kit consists of 349 amino acid residues. The average protein kinase domain contains about 275 residues and the larger size of Kit is due to the inclusion of a kinase insert domain (KID) of 77 residues. Based upon the amino acid sequences of about five dozen protein-tyrosine and protein-serine/threonine kinases, Hanks and Hunter partitioned protein kinases into 12 domains (I-VIA, VIB-XI) [39]. Domain I of Kit contains a glycine-rich loop (GRL) with a GxGxΦG signature (^{596}GAGAFG^{601}), where Φ refers to a hydrophobic residue and is phenylalanine in the case of Kit. The glycine-rich loop connects the β1- and β2-strands that make up part of the roof of the ATP-binding site. The flexible glycine-rich loop permits both ATP binding and ADP release during the catalytic cycle. Domain II of Kit contains a conserved Ala-Xxx-Lys (^{621}AVK^{623}) sequence in the β3-strand and domain III contains a conserved glutamate (E640) in the αC-helix that forms a salt bridge with the conserved β3-lysine in all active protein kinases (Fig. 2A) and many dormant protein kinase conformations (Fig. 2D). Domain V of Kit contains a ^{671}EYCCYG^{676} hinge that connects the small and large lobes.

Domain VIB within the large lobe of Kit contains a conserved HRD sequence, which forms part of the catalytic loop (^{790}HRDLAARN^{797}).

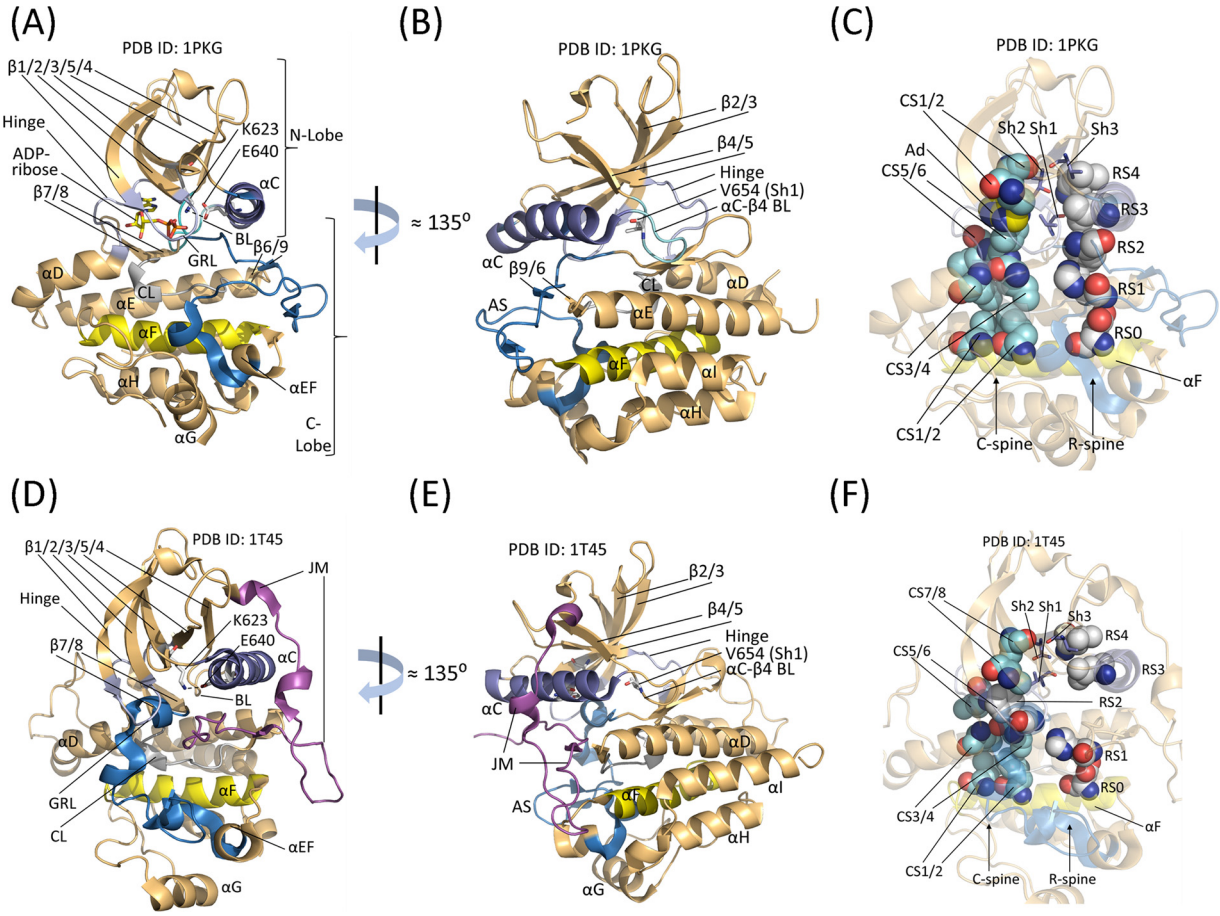

Fig. 2. Overview of the structures of active Kit (A and B), DFG-D_{in} Kit spine and shell residues (C), inactive Kit (D and E), and DFG-D_{out} Kit spine and shell residues (F). Ad, adenine; AS, activation segment (blue); BL, back loop; CL, catalytic loop; CS, catalytic spine; GRL, glycine-rich loop; JM, juxtamembrane segment; RS, regulatory spine; Sh, Shell. All figures except for 1, 7, and 9 were prepared using the PyMOL Molecular Graphics System Version 1.5.0.4 Schrödinger, LLC.

Kit domain VII contains an ^{810}DFG^{812} signature and domain VIII contains an ^{837}APE^{839} sequence, which represent the beginning and end of the Kit activation segment. This 30-residue segment exhibits different conformations in the active and dormant states. The remaining domains (IX–XI) form the αE–αI helices (Fig. 2B and E). The X-ray crystallographic structure of the catalytic subunit of protein kinase A (PKA) generated an invaluable blueprint for formulating the roles of the 12 Hanks domains and the structure has illuminated the underlying biochemistry of the entire protein kinase enzyme superfamily (PDB ID: 2CPK) [40,41]. All protein kinases possess a small N-terminal and a large C-terminal lobe that are connected by the hinge segment [2]. The N-terminal lobe contains five conserved β-strands (β1–5) and an important regulatory αC-helix and the C-terminal lobe of active enzymes contains seven helices (αD–αI and αEF) along with four conserved β-strands (β6–β9) (Fig. 2). Of the many hundreds of protein kinase structures that have been described, all of these contain the original protein kinase fold as observed first in PKA [2,40,41].

All catalytically active protein kinases contain a K/E/D/D (Lys/Glu/Asp/Asp) amino acid signature necessary for protein kinase catalysis (Table 2) [2]. The lysine and glutamate occur within the small amino-terminal lobe and the two aspartate residues occur within the large carboxyterminal lobe. ATP binds in the cleft between the two lobes and interacts with each. Comprehensive analyses indicate that an electrostatic bond between the β3-lysine and the αC-glutamate is required for the formation of an active protein kinase conformation, which corresponds to an "αC_{in}" arrangement as shown for active Kit (Fig. 2A). These residues in many dormant enzymes fail to form this electrostatic bond and thereby form an inactive "αC_{out}" structure (See Refs. [2] for details). The αC_{in} configuration is necessary, but not sufficient, for the expression of enzymatic activity. Although the β3-K623 and αC-E640 of dormant Kit form an electrostatic bond (Fig. 2D), molecular measurements indicate that this corresponds to an αC-dilated conformation as described later in this Section. Moreover, the activation segment of dormant Kit is in a closed conformation that blocks protein/peptide and ATP binding. The proximal portion of the closed activation segment of Kit contains an inhibitory α-helix. The activating GIST D816V mutation [22] occurs within this segment and this mutation may destabilize the dormant enzyme leading to enzyme activation.

The large C-terminal lobe contains catalytic loop residues within domain VIb that plays essential structural and catalytic roles. Furthermore, two Mg^{2+} ions have been demonstrated to participate during each catalytic cycle of several protein kinases [42,43] and two Mg^{2+} ions are presumably required for the proper functioning of Kit. By inference, Kit D792 (the catalytic loop HRD-D792) and the first D of K/E/D/D) binds to Mg^{2+}(1), which in turn binds to the β- and γ-phosphates of ATP. In the active conformation, the DFG-D is directed inward toward the active site as depicted in Fig. 3A. In contrast, the DFG-D of inactive Kit is pointed outward producing an inactive DFG-D_{out} structure (Fig. 3B). Note that the Kit X-ray crystallographic structure (PDB ID: 1T45) was obtained in the absence of any drug so that one cannot argue that a drug induces the DGF-D_{out} conformation.

Vijayan et al. inspected the structures of about 200 hundred protein kinases and they allocated the DFG-D_{out} structures into (i) classical and (ii) nonclassical groups [44]. This distinction was necessary owing to the variations in the locations of the activation segment DFG-D and DFG-F in the eukaryotic kinome. They devised two measurements that

Table 2
Important residues in human Kit.[a]

	Kit	Inferred function	Hanks no.
UniProtKB accession no.	P10721		
No. of residues	976		
Molecular Wt (kDa)[b]	110		
Signal sequence	1–25		None
Extracellular domain	26–524		None
D1	27–112	SCF binding	None
D2	121–205	SCF binding	None
D3	212–308	SCF binding	None
D4	317–410	Promotes receptor dimer formation	None
D5	413–507	Promotes receptor dimer formation	None
TM segment	525–545	Links extracellular and intracellular domains and mediates receptor dimer formation	None
JM segment	546–588	Regulatory and signaling roles	None
JM segment tyrosine phosphorylation sites	568, 570	Signal transduction	None
Protein kinase domain	589–937	Catalyzes substrate transphosphorylation	I–X1
Glycine-rich loop	^{596}GAGAFG^{601}	Anchors ATP β-phosphate	I
β3-K of K/E/D/D	K623	Forms salt bridges with ATP α- and β-phosphates and with αC-E	II
αC-E, E of K/E/D/D	E640	Forms salt bridges with β3-K	III
Hinge residues	^{671}EYCCYG^{676}	Connects N- and C-lobes and hydrogen bonds with the ATP adenine	V
Kinase insert domain	685–761	Signal transduction	None
Kinase domain tyrosine phosphorylation sites	703, 721, 730	Interact with a variety of docking proteins that mediate intracellular signaling	
Catalytic loop, HRDLAARN	790–797	Plays both structural and catalytic functions	VIb
Catalytic loop HRD-D, First D of K/E/D/D	D792	Catalytic base (abstracts protein substrate proton)	VIb
Catalytic loop Asn, HRDLAARN	N797	Chelates Mg^{2+}(2)	VIb
AS DFG-D, Second D of K/E/D/D	D810	Chelates Mg^{2+}(1)	VII
AS	810–839	Positions protein substrate	VII–VIII
AS tyrosine phosphorylation site	Y823	Stabilizes the AS after phosphorylation	VIII
End of AS	^{837}APE^{839}	Interacts with the αHI loop and stabilizes the AS	VIII
C-terminal tail	938–976	Signal transduction	None
C-terminal tail tyrosine phosphorylation sites	900, 936	Mediate intracellular signaling	None

[a] AS, activation segment; D1, Immunoglobulin-like domain 1; JM, juxtamembrane; TM, transmembrane.
[b] Unprocessed and non-glycosylated gene product.

differentiated these groups and labeled them D1 and D2. D1 is the distance between the αC-atoms of the DFG-F of the activation segment and the HRDLxxxxN asparagine at the end of the catalytic loop and D2 is the distance between the αC-atoms of the DGF-F and the αC-E residue. The enzyme possesses a classical DFG-D_{out} structure provided that D1 is less than 7.2 Å and D2 is greater than 9 Å. In the case of the structure of dormant Kit (PDB:ID 1T45), D1 equals 5.6 Å and D2 equals 12.1 Å (Fig. 3B); accordingly, this is within the classical DFG-D_{out} group. The structure of active Kit (PDB ID: 1PKG) shows D1 and D2 values of 9.0 Å and 4.9 Å that are inconsistent with a classical DFG-D_{out}, but these values are consistent with the DFG-D_{in} classification (Fig. 3A). The relative location of the β3-strand and αC-helix is an important structural parameter. The electrostatic bond between β3-K and αC-E is broken in the inactive αC_{out} configuration. However, Vijayan et al. reported that this salt bridge occurs in ≈ 90% of classical DFG-D_{out} structures and they call these αC-dilated structures to differentiate them from αC_{in} configurations [44]. These investigators measured the distance from the α-carbon atoms of the DFG-D and αC-E, which we have called D3, and found that a D3 value of less than 9 Å represents the αC_{in} structure while those with a D3 value greater than 10.5 Å represents an αC_{out} configuration. In the case of the epidermal growth factor receptor (EGFR) αC_{out} structure, D3 is 12.3 Å. The αC-dilated structure has a D3 value between 9 Å and 10.5 Å (Fig. 3B). In the case of dormant Kit (PDB ID: 1T45) the D3 value is 10.0 Å and represents the αC-dilated structure. The distance between the β3-lysine ε-amino group and αC-glutamate carboxyl group is 4.3 Å in the αC-in structure (PDB ID: 1PKG), 2.6 Å in the αC-dilated structure (1T46), and 13.3 Å in the αC_{out} structure (4HJO).

The 6-amino nitrogen of ADP/ATP forms a hydrogen bond with the carbonyl backbone residue of the first Kit hinge residue (E671) that connects the small and large lobes of the protein kinase domain and the *N*1 nitrogen of the adenine base forms a second hydrogen bond with the N−H group of the third hinge residue (C673). The adenine binding pocket is located next to these hinge residues. As noted later, most orally effective small-molecule steady-state ATP competitive inhibitors of protein kinases, including Kit, make one or more hydrogen bonds with the backbone residues of the connecting hinge.

The protein kinase activation segment, which is typically 20–30

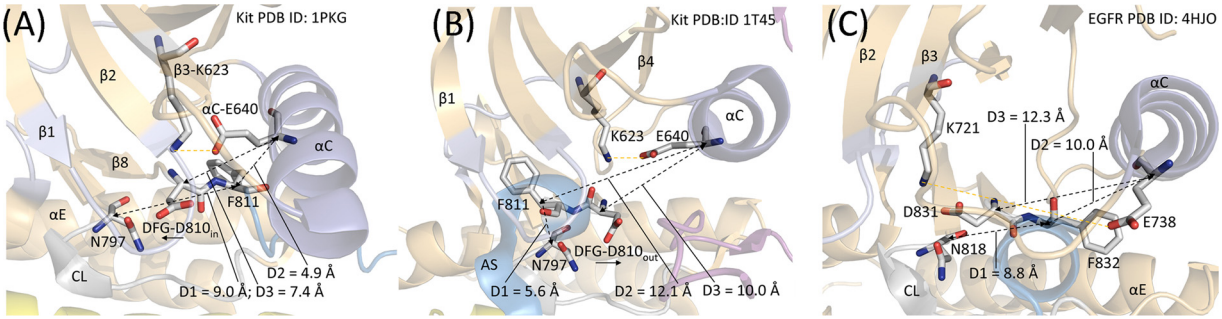

Fig. 3. (A) Active Kit with αC-in and DGF-D_{in}. (B) Inactive αC-dilated Kit with DFG-D_{out}. (C) Inactive EGFR with αC-helix out and DFG-D_{in}. AS, activation segment; CL, catalytic loop.

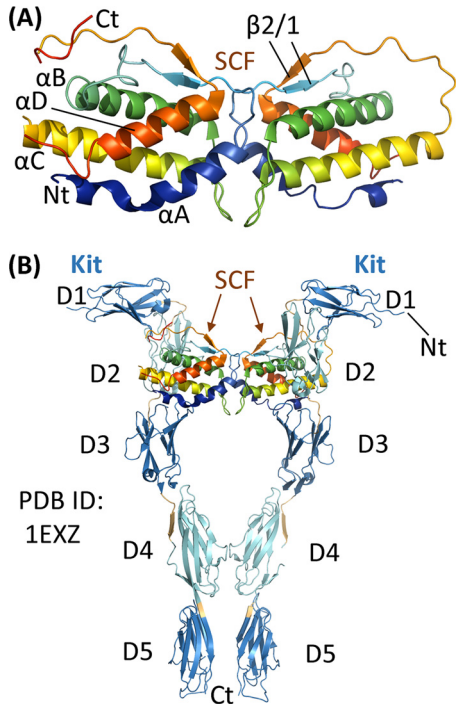

Fig. 4. (A) Stem cell factor head-to-head dimer in its Kit-binding conformation as seen in (B). (B) The SCF dimer bound to the Kit dimer. Ct, carboxyterminus; D1, immunoglobulin-like domain 1; Nt, amino-terminus.

residues in length, plays an important role in the catalytic cycle [45]. The origin of the segment is located near the αC-helix and the conserved HRD of the catalytic loop. These components are linked by hydrophobic interactions as described in Section 3.2 as part of the regulatory spine. With most protein kinases, phosphorylation of one or more residues within the activation segment converts a dormant to a catalytically active enzyme [46,47]. Although Kit contains an appropriately positioned tyrosine within the activation loop (Y823), its phosphorylation is not required for enzyme activation, but its phosphorylation is required for physiological signaling [48]. Lemmon and Schlessinger reviewed the mechanisms for receptor protein-tyrosine kinase activation and this process generally requires growth factor-induced formation of receptor dimers and subsequent protein kinase activation or it involves the growth factor-induced activation of preformed dimers, which occurs during the activation of the insulin receptor [14]. Under physiological conditions, SCF binds to D1/2/3 of two monomers to promote receptor dimerization [49,50]. This binding has a zipper effect and brings D4, D5, and the transmembrane segments of two receptor monomers together (Fig. 4). Following this process, one member of the dimer pair catalyzes the phosphorylation of the tyrosine residues within the inhibitory JM domain of the receptor partner (in *trans*) along with the phosphorylation of other protein-tyrosines that creates docking sites for signal transduction proteins. Phosphorylation of the JM domain relieves inhibition and promotes activation. Activation segment tyrosine phosphorylation occurs late in this process and is not directly related to Kit activation. In addition to the activation segment, Kit is autoinhibited by the JM segment. DiNitto et al. reported that phosphorylation of Y568 and Y570 within the JM segment contributes to Kit activation and these phosphorylation reactions occur prior to activation segment Y823 phosphorylation [48].

The Kit HRDLAARN catalytic-loop aspartate (D792), which is the first D of the K/E/D/D signature, functions as a base and removes a proton from the protein-tyrosine−OH group thereby enabling the nucleophilic attack of −O: onto the γ-phosphorus atom of ATP (Fig. 5) [51]. The activation segment, when it is in its open conformation, helps to position the protein substrate. β3-K623 forms salt bridges with αC-

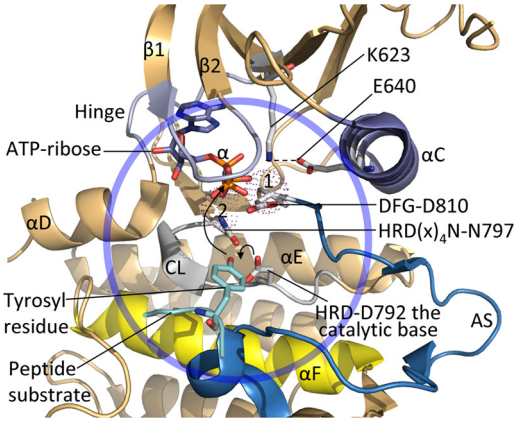

Fig. 5. Inferred mechanism of the Kit-catalyzed protein kinase reaction. HRD-D792 abstracts a proton from the protein tyrosyl substrate allowing for its nucleophilic attack onto the γ-phosphorus of ATP. The chemistry occurs within the circle. 1 and 2 label the two Mg^{2+} ions shown as dots. AS, activation segment; CL, catalytic loop; The figure was prepared from FGFR2 (PDB ID: 2PVF), but the residue numbers correspond to those of human Kit.

E640 and the α- and β-phosphates of ATP. Extrapolating from PKA [2,43], Mg^{2+}(1) and DFG-D810 bind to the β- and γ-phosphates while Mg^{2+}(2) and β3-K623 bind to the α- and β-phosphates of ATP thereby aiding catalysis. The catalytic segment AAR sequence occurs in many receptor protein-tyrosine kinases including colony-stimulating factor-1 receptor, Flt3, Kit, PDGFRα/β, and EGFR while RAA occurs in many nonreceptor protein-tyrosine kinases such as Src [39]. However, the structural or functional significance of this difference in the catalytic loop is unclear.

Under physiological conditions, the activity of protein kinases and downstream signaling events are stringently regulated. Binding of SCF to Kit leads to receptor mediated endocytosis and degradation of the ligand-receptor complex in endosomes; both the ligand and receptor are degraded following fusion with lysosomes [9]. Moreover, activated receptors undergo ubiquitylation, a process that targets them for degradation in proteasomes. The internalization rate of the Kit is dependent on its protein kinase activity. Phosphorylated Y568 binds Src protein-tyrosine kinase, and Src may be required for Kit degradation [52].

In addition to receptor endocytosis, protein-tyrosine phosphatase activity directed against the receptor and downstream proteins negatively affect Kit signaling [8]. The protein phosphatase superfamily is large and consists of about 100 gene products [5]. The largest phosphatase family member employs an active-site cysteine sulfhydryl group as a nucleophile that attacks the phosphate group of the substrate. Shp1 and Shp2 phosphatases, two members of this family that are able to catalyze the hydrolysis of pTyr and lipid phosphoinosotides, negatively modulate Kit signaling. These enzymes, which catalyze the hydrolysis of Kit receptor phosphotyrosines, are classical cysteine-based nonreceptor, or cytosolic, protein tyrosine phosphatases. In contrast, receptor protein-phosphatases are plasma membrane-bound enzymes that interact with extracellular molecules such as proteoglycans and antigen receptors [53].

Kit signaling resembles that of other receptor protein-tyrosine kinases [2]. For example, Grb2 interacts with pY703 and pY936, which leads to the downstream activation of the Ras/Raf/MEK/ERK map kinase pathway that regulates cell division and cell survival [8,9]. Moreover, Kit activates the related p38, JNK (c-Jun N-terminal kinase), and ERK5 signaling modules. Additionally, Src family kinases interact with pY568 and pY570; these phosphorylation sites displace the Src inhibitory pY530 residue from the Src SH2 domain resulting in enzyme activation [42,54–56]. Src is upstream of the map kinase, AKT/PKB, and signal transducer and activator of transcription-3 (STAT3)

pathways [42,57]. The signaling of Src with EGFR, fibroblast growth factor receptor, insulin-like growth factor receptor, Kit, c-Met, and PDGFRα/β is stringently regulated and bidirectional. Furthermore, the regulatory subunit of phosphatidylinositol 3′-kinase binds to pY721 and pY900 leading to the activation of AKT/PKB thereby promoting cell survival. Finally, phospholipase Cγ binds to pY730 leading to the activation of PKC with attendant effects on cell proliferation and survival. See Ref. [9] for a comprehensive discussion of Kit signal transduction.

3.2. The hydrophobic spines of Kit

Kornev et al. investigated the structures of 23 protein kinases and they ascertained the role of several essential residues by a local spatial pattern alignment algorithm [58,59]. They grouped together (i) four hydrophobic residues as a regulatory or R-spine and (ii) eight hydrophobic residues as a catalytic or C-spine. Each spine contains amino acid residues from both the amino-terminal and carboxyterminal lobes. The R-spine contains one residue from the regulatory αC-helix and another from the activation segment (DFG-F), both of which are major components that may assume more active and less active conformations. The base of the R-spine within the large lobe anchors the catalytic loop and activation segment in an active state and the C-spine positions ATP within the active site cleft to enable catalysis. Furthermore, the correct alignment of both spines is necessary for the assembly of an active enzyme as described for the ALK receptor protein-tyrosine kinase, the cyclin-dependent protein kinases, EGFR, ERK1/2, the Janus kinases, MEK1/2, PDGFRα/β, RET, ROS1, Src, and VEGFR1/2/3 [23,42,60–69].

Going from the bottom to the top, the protein kinase R-spine consists of the catalytic loop HRD-H, the activation loop DFG-F, an amino acid four residues carboxyterminal to the conserved αC-glutamate, and a hydrophobic amino acid at the beginning of the β4-strand [58]. The backbone N—H group of the HRD-H forms an electrostatic bond with an invariant aspartate carboxylate group within the αF-helix. Again, going from the bottom to the top of the R-spine, Meharena et al. designated the R-spine residues as RS0, RS1, RS2, RS3, and RS4 (Fig. 2C) [70]. The R-spine of active Kit with DFG-D_{in} is linear (Fig. 2C). In contrast, the R-spine of dormant enzymes such as Kit with DFG-D_{out} is nonlinear and broken with a displaced RS2 residue (Fig. 2F) (See Refs. [2,71] for details). The protein kinase C-spine contains amino acid residues from both the amino-terminal and carboxyterminal lobes; the adenine base of ATP completes this spine (Fig. 2C) [59]. The two residues of the amino-terminal lobe that interact with the ATP adenine include an invariant valine at the beginning of the β2-strand (CS7) and the conserved alanine from the signature AxK of the β3-strand (CS8). Furthermore, a residue from the β7-strand (CS6) on the floor of the adenine pocket interacts hydrophobically with the ATP. Based upon the observation of dozens of crystal structures, essentially all steady-state ATP-competitive protein kinase antagonists interact with CS6. The CS6 residue occurs between two hydrophobic residues (CS4 and CS5) that constitute the β7-strand and CS6 interacts with the CS3 residue near the beginning of the αD-helix of the carboxyterminal lobe. CS5/6/4 immediately follow the catalytic loop asparagine (HRDxxxxN) so that these residues can be determined easily from the primary structure. To complete the C-spine, the CS3 and CS4 residues interact hydrophobically with CS1 and CS2 of the αF-helix (Fig. 2C and F) [59]. The αF-helix, which spans the entire carboxyterminal lobe, anchors both the R- and C-spines. Moreover, both spines play an essential role in anchoring the protein kinase catalytic residues in an active state. CS7 and CS8 in the N-terminal lobe make up part of the “ceiling” of the adenine-binding pocket while CS6 in the C-terminal lobe makes up part of the “floor” of the binding pocket.

Based upon the results of site-directed mutagenesis experiments, Meharena et al. characterized three shell (Sh) residues in the PKA catalytic subunit that support the R-spine, which they designated as Sh1, Sh2, and Sh3 [70]. The Sh2 residue represents the canonical gatekeeper residue of protein kinases. The gatekeeper plays an essential role in controlling access to the back pocket [72,73] or hydrophobic pocket II (HPII) [73,74]. In contrast to the identification of the HRD, DFG, or APE signatures, which is based upon the primary structure [39], the two spines were identified by their spatial locations in active or inactive protein kinases [58,59]. Table 3 provides a compilation of the spine and shell residues of Kit and PKA. Small molecule protein kinase inhibitors often interact with residues within the C-spine as well as with R-spine and shell residues [71].

Table 3
Spine and shell residues of human Kit and murine PKA.

	Symbol	KLIFS No.[a]	Kit	PKA[b]
Regulatory spine				
β4-strand (N-lobe)	RS4	38	L656	L106
C-helix (N-lobe)	RS3	28	L644	L95
Activation loop F of DFG (C-lobe)	RS2	82	F811	F185
Catalytic loop His/Tyr (C-lobe)	RS1	68	H790	Y164
F-helix (C-lobe)	RS0	None	D851	D220
R-shell				
Two residues upstream from the gatekeeper	Sh3	43	V668	M118
Gatekeeper, end of β5-strand	Sh2	45	T670	M120
αC-β4 loop	Sh1	36	V654	V104
Catalytic spine				
β3-AxK motif (N-lobe)	CS8	15	A621	A70
β2-strand (N-lobe)	CS7	11	V603	V57
β7-strand (C-lobe)	CS6	77	L799	L173
β7-strand (C-lobe)	CS5	78	L800	I174
β7-strand (C-lobe)	CS4	76	I798	L172
D-helix (C-lobe)	CS3	53	L678	M128
F-helix (C-lobe)	CS2	None	L862	L227
F-helix (C-lobe)	CS1	None	F858	M231

[a] KLIFS (kinase–ligand interaction fingerprint and structure) from Ref. [88].
[b] From Refs. [58,59,70].

Mol et al. determined the X-ray structure of the active form of Kit (PDB ID: 1PKG) [75]. The DFG-D is pointed inward toward the active site, the configuration of the αC-helix is in its active αC_{in} configuration with E640 forming a hydrogen bond with the β3-K623, the activation segment is in the open conformation, and the catalytic and regulatory spines are linear and are neither bent nor broken. In the case of dormant Kit (PDB ID: 1T45) [76], the X-ray structure shows that the autoinhibitory juxtamembrane segment blocks ATP and peptide substrate binding. Moreover, the JM Y553 forms a salt bridge with E640 of the αC-helix thereby immobilizing it. Additionally, the activation segment is in its closed inactive DFG-D_{out} conformation and the structure is that of an inactive protein kinase with a broken R-spine (Fig. 2F).

3.3. Properties of mutant Kit receptors

Somatic mutations in the D5 extracellular domain are oncogenic and lead to the pathogenesis of core-binding factor AML, GIST, and mastocytosis (Table 1). Shi et al. divided *KIT* mutations into class I and II groups [50]. Class I mutants as defined by Shi et al. [50] − which include the D5 D419A and N505I point mutations, deletion of Y418 and D419, or duplication of A502/Y503–occur within D5 and are expressed within the plasma membrane and display increased sensitivity to SCF. They have a long half-life in unstimulated cells, but are subject to SCF-induced internalization, ubiquitinylation, and proteolysis. In contrast, class II mutants such as T417IΔ418–419 within D5 and V560D and D816V and the V560D/Y823D double mutant in the protein kinase domain have constitutively activated tyrosine kinase activities and exhibit low or miniscule surface expression. These mutants undergo rapid SCF-independent internalization, ubiquinylation, and proteolysis. It is possible to inhibit class I mutants with antibodies directed against the extracellular domain. Owing to their intracellular location, the antibody-targeting strategy would be ineffective in class II mutants.

Gajiwala et al. found that Kit bearing mutations in the activation segment undergo autoactivation much more rapidly than wild type Kit [77]. Such primary activating mutations occur in core-binding AML, mastocytosis, and seminoma, but not in GIST. However, secondary imatinib-resistant mutations in GIST commonly involve the activation segment. It is unclear whether secondary drug-resistant mutations are present prior to any anti-Kit therapy or whether they emerge *de novo* during treatment [31]. Activation segment mutations such as D816H destabilize the inactive enzyme (DFG-D_{out} conformation) and shift the equilibrium towards the DFG-D_{in} conformation with an open activation segment.

Gajiwala et al. demonstrated that imatinib, which binds preferentially to the DFG-D_{out} enzyme state, is not effective against the D816H/V mutants nor the V560D/T760I double mutant [77]. Garner et al. found that the *KIT* V654A mutant and the V559D/V654A double mutant are resistant to imatinib but are sensitive to sunitinib [78]. V654 is the Sh1 residue in the back loop. These investigators hypothesize that the interaction of imatinib with V654 is required for high-affinity binding. In contrast, sunitinib does not extend into the back loop and its binding is independent of V654. Gajiwala et al. performed steady-state kinetic studies on the wild type and V654A Kit mutant [77]. They observed that the ATP K_m value of the mutant was about one-third that of the wild type enzyme (13.5 μM vs. 42.5 μM) and the V_{max} values were similar (1.26 s^{-1} for the mutant vs 1.67 s^{-1} for the wild type enzyme). Owing to the change of the more hydrophobic valine to alanine, one might have expected that the Sh1 mutant enzyme would have had impaired activity.

The T760I gatekeeper (Sh2) mutation is an acquired secondary-resistance mutation and does not occur as a primary activating mutation (Table 1). Kissova et al. compared the steady-state enzyme kinetics of the Kit wild type and the T670I mutant [79]. They found that the mutation decreased the K_m value for ATP from 6.6 μM for the wild type enzyme to 0.56 μM. As a consequence, ATP-competitive drugs would be less able to bind and inhibit the enzyme. They also reported that the wild type enzyme had a 25-fold higher K_m for an artificial peptide substrate. The conversion of threonine to isoleucine has at least two effects in producing decreased imatinib affinity. As noted in Section 4, imatinib forms a hydrogen bond with the −OH group of the gatekeeper and isoleucine lacks a hydrogen-bond acceptor. Second, the larger isoleucine can block access to the back pocket by ligands such as imatinib. In addition to its larger size, isoleucine is a hydrophobic shell residue that may strengthen the catalytic spine as compared to threonine and accordingly isoleucine may increase catalysis.

Many of the activating mutations, especially those occurring in GIST, are found in the inhibitory juxtamembrane segment (Table 1). As a consequence, these mutations may destabilize this inhibitory segment and lead to enzyme activation. The most common juxtamembrane exon 11 mutations include V559D and V560D. These valine residues interact hydrophobically with ^{569}VYI^{571} within the JM segment and Y646 within the αC-helix. Conversion to the charged aspartate would be expected to disrupt these interactions. V560 interacts hydrophobically with V569, Y570, and N787 and a mutation to glycine that occurs in mastocytosis is expected to result in the loss of these contacts resulting in enzyme activation. Several activating mutations occur within the important regulatory activation segment, which occurs in an autoinhibited state in the dormant enzyme. D816 occurs within an activation segment α-helix in the dormant enzyme and its hydrophilic side chain extends into the solvent (PDB ID: 1T45). Its mutation to hydrophobic valine, phenylalanine, or tyrosine would disfavor extension into the solvent and thereby shift the equilibrium toward an open activation segment and enzyme activation. The activation segment D816 is conserved among many receptor protein-tyrosine kinases; it occurs within all five members of the type III receptor family as well as the VEGFR and fibroblast growth factor receptor families.

Imatinib, sunitinib, and sorafenib are predominantly type II inhibitors that bind to the DFG-D_{out} inactive enzyme [71]. Several of the secondary-resistance mutations occur within the JM module that may lead to enzyme activation and insensitivity to type II inhibitors. Similarly, several secondary-resistance mutations occur within the activation segment and promote the conversion to an active enzyme. K642 occurs within the JM module and forms a hydrogen bond with the −OH group of T574, also within the JM segment. Conversion to a glutamate residue would disrupt this interaction. The location of a protein kinase mutation often gives a clue for the basis of an observed change in activity. When the effects of such mutations are studied directly, it is possible that multiple distinct and complementary mechanisms are actually responsible for the observed activity changes and the mechanisms are not as simple as hypothesized here. The location of these mutations is depicted in Fig. 6.

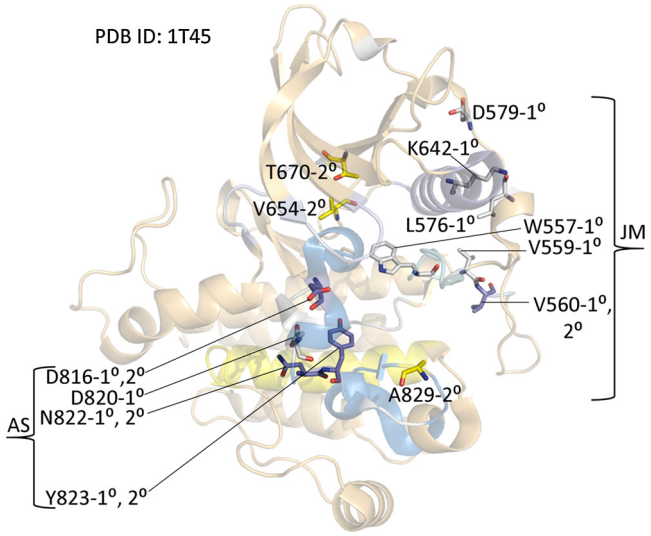

Fig. 6. Location of primary (1°) activating mutations, secondary (2°) resistance mutations, or both (1°, 2°). AS, activation segment; JM, juxtamembrane segment.

4. FDA-approved Kit inhibitors

4.1. Classification of protein kinase-drug complexes

Dar and Shokat described three classes of small molecule protein kinase inhibitors and labeled them types I, II, and III [80]. The type I antagonists bind within the ATP pocket of an active protein kinase domain; the type II antagonists bind to an inactive protein kinase domain with the activation segment DFG-D pointing away from the active site (DFG-D_{out}) while the type III antagonists bind at an allosteric site, which is not part of the active site [81] and is outside of the ATP-binding pocket. Subsequently, Zuccotto defined type I½ antagonists as drugs that bind to an inactive protein kinase domain with the DFG-D pointed inward (DFG-D_{in}) toward the active site (in contrast to the DFG-D_{out} conformation) [82]. The inactive enzyme may exhibit a closed activation segment, a nonlinear or broken regulatory spine, or an αC-$helix_{out}$ conformation. In a subsequent paper, Gavrin and Saiah divided allosteric inhibitors into two types: III and IV [83]. Accordingly, type III antagonists bind within the cleft between the small and large lobes next to, but independent of, the ATP binding site while type IV allosteric antagonists bind elsewhere. Furthermore, Lamba and Gosh defined bivalent inhibitors as those antagonists that span two distinct parts of the protein kinase domain as type V inhibitors [84]. For example, an antagonist that binds to the ATP-binding site and the peptide substrate site would be classified as a type V inhibitor. To complete this grouping, we classified antagonists that bind covalently with the target enzyme as type VI inhibitors [71]. For example, afatinib is a covalent type VI inhibitor of EGFR that is FDA-approved for the treatment of non-small

cell lung cancer. Mechanistically, this medicinal binds initially to an active EGFR conformation (like a type I inhibitor) and then the thiol group of EGFR C797 attacks the drug to form a covalent adduct [71].

Because of the diversity of dormant protein kinase conformations when compared with the conserved more active conformation, it was hypothesized that type II drugs would be more selective than type I drugs which bind to the canonical active conformation. The analysis of Vijayan et al. support this hypothesis [44] while that of Zhao et al. and Kwarcinski et al. does not [30,85]. Type III allosteric inhibitors bind adjacently to the adenine binding pocket [83]. Owing to the greater variability in this region when compared with the ATP binding pocket, type III inhibitors may be more selective than type I, I½, or II inhibitors. Experiments by Kwarcinski et al. suggest that inhibitors that bind to the αC_{out} conformation may be more selective than the traditional type I and II inhibitors [85]. FDA-approved αC_{out} inhibitors include lapatinib, an EGFR/ErbB1 and ErbB2/HER2 antagonist, and neratinib, an ErbB2/HER2 antagonist, both of which are used in the treatment of breast cancer. However, their studies indicate that not all protein kinases are able to assume the αC_{out} conformation while they suggest that all kinases are able to assume the DFG-D_{out} conformation.

We previously divided the type I½ and type II antagonists into A and B subtypes [71]. As described in Section 4.3, imatinib is a type II inhibitor of Kit (PDB ID: 1T46). This medication binds to the protein kinase domain with the DFG-D_{out} configuration and extends into the back cleft. We classified antagonists that extend into the back cleft as type IIA inhibitors. In contrast, we classified antagonists such as sunitinib that (i) bind to Kit DFG-D_{out} conformation and (ii) do not extend into the back cleft as type IIB inhibitors (PDB ID: 3G0E). Based on incomplete data, the potential significance of this difference is that type A inhibitors bind to their target kinase with a long residence time when compared with type B antagonists.

Type II antagonists bind to their target enzyme with the DFG-D pointing away from the active site [71,86,87] and they are usually the easiest to identify. As a result, the DFG-D and DFG-F switch positions and the change in location of the phenylalanine creates a large allosteric pocket that interacts with fragments of type II inhibitors such as imatinib. The ATP/ADP binding site occurs within the front pocket and does not extend past the gate area into the back pocket. In section 4.3, we will see that the Kit antagonists studied in this paper, with the exception of midostaurin, are type II inhibitors.

4.2. Drug-ligand binding pockets

Liao [74] and van Linden et al. [88] divided the cleft between the protein kinase small and large lobes into a front cleft or pocket, a gate area, and a back cleft. The back pocket or hydrophobic pocket II (HPII) includes the gate area and back cleft (Fig. 7). The front cleft includes the glycine-rich loop, the hinge residues, the linker connecting the hinge residues to the large lobe αD-helix, and the amino acid residues within the catalytic loop (HRDxxxxN). The gate area includes the β3-strand and the beginning of activation segment including DFG. The back cleft extends to the αC-helix, the αC-β4 back loop, portions of the β4- and β5-strands, and a section of the αE-helix.

van Linden et al. defined several sub-pockets that are included in these three regions [88]. Accordingly, the front cleft contains an adenine-binding pocket (AP) next to two front pockets (FP-I and FP-II**).** FP-I occurs between the solvent-exposed linker connecting the hinge residues to the αD-helix and the xDFG-motif (where x is the residue before the activation segment DFG) and FP-II is located between the glycine-rich loop and the β3-strand on top of the cleft. Back pocket I (BP-I) is located in the gate area between the xDFG-motif, the β3- and β4-strands, the conserved β3-K of the AxK signature, and the αC-helix. BP-I can be divided into two subpockets (BP-I-A and BP-I-B). The smaller BP-I-A is found at the top of the gate area and is formed by residues of the β3- and β5-strands including β3-AxK along with the αC-helix. The larger BP-I-B occurs in the center of the gate area allowing access to the back cleft. BP-I-A and BP-I-B are found in both DFG-D_{in} and DFG-D_{out} conformations

BP-II-A-in and BP-II-in occur in the DFG-D_{in} conformation within the back cleft [74]. These pockets are bounded by the DFG-motif, the αC-helix, the αC-β4 back loop, and the β4- and β5-strands. Considerable adjustment of BP-II-A-in and BP-II-in occurs to produce BP-II-out in the DFG-D_{out} conformation; this modification is associated with the change in the location of DFG-F. The resulting compartment is labeled back pocket II-out (BP-II-out); it occurs where the DFG-F is found in the DFG-D_{in} conformation. BP-II-B is bounded by the αC-helix and β4-strand in both DFG-D_{in} and DFG-D_{out} conformations. Back pocket III (BP-III) occurs only in the DFG-D_{out} conformation. This compartment is located on the floor of BP-II-out between the DFG-D_{out} motif, the αC-β4 back loop, the αC- and αE-helices, the β6-strand, and the conserved catalytic loop HRD-H. Two somewhat hydrophobic back pockets (BP-IV and BP-V) occur between the αC-helix, the DFG-D_{out} motif, the catalytic loop, the β6-strand, and the activation segment (Fig. 7). These two pockets are partially solvent exposed.

The Kit multikinase inhibitors including imatinib are found within a box that is made up of nearly 30 Kit amino acid residues. For example, L799 (CS6), the C809, D810, and F811 of the xDFG motif, and residues before and within the catalytic loop including C788, I789, H790, and R791 occur on the bottom of drug-binding pocket as illustrated in Fig. 8. L799 is beneath, the xDFG motif is in front, C788 and I799 are

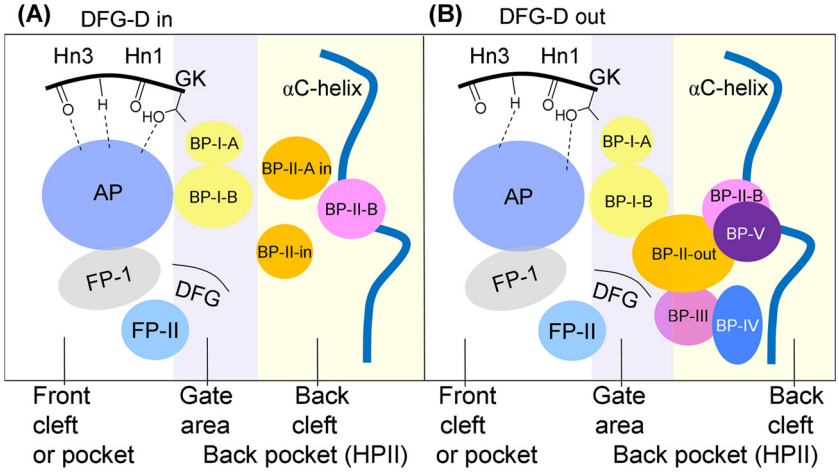

Fig. 7. Location of the protein kinase domain drug-binding pockets. AP, adenine pocket; BP, back pocket; FP, front pocket; Hn, hinge; HPII, hydrophobic pocket II. Adapted from Refs. [74,88].

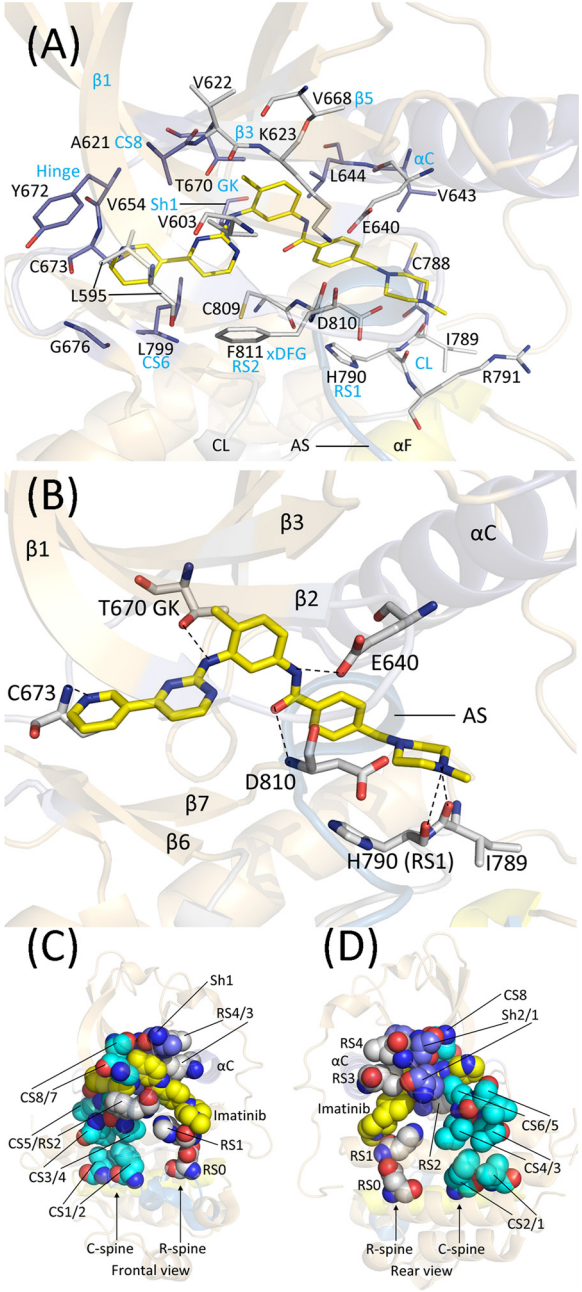

Fig. 8. (A) Overview of the drug binding site of Kit. Sticks with blue carbon atoms are behind imatinib and those with gray carbon atoms are in front of imatinib. (B) Structure of the Kit-imatinib complex. Kit spine-imatinib interaction – frontal view (C) and rear view (D). The imatinib carbon atoms are colored yellow; C-spine, cyan; R-spine, gray; Shell residues, blue. AS, activation segment; CL, catalytic loop; GK, gatekeeper. The dashed lines depict polar bonds.

behind, and H790 and R791 are in front of the drug as depicted. The hinge residues Y672 and C673 occur on the left and the β3-A621, V622, and K623 occur in the ceiling of the box. A621 is above imatinib and V622 and K623 occur in front of the drug. The αC-E640, V643, and L644 occur on the right upper portion of the box while the β2-V603 occurs in front of the drug and the back-loop V654 occurs in back of the antagonist. Additionally, E640 is in front of the drug and V622 and K623 are behind it. The T670 gatekeeper occurs at the end of the β5-strand and is in the back of the drug-binding pocket while L595 occurs on the left at the end of the β1-strand and in front of the drug.

4.3. Structures of Kit-drug complexes

Imatinib (4-[(4-methylpiperazin-1-yl)methyl]-*N*-[4-methyl-3-[(4-pyridin-3-ylpyrimidin-2-yl)amino]phenyl]benzamide) (Fig. 9A) is a Kit multikinase inhibitor that is FDA-approved for the first-line treatment of Ph^+ chronic myelogenous leukemia, chronic eosinophilia leukemia, dermatofibrosarcoma protuberans, hypereosinophilic syndrome, Kit-mutation positive GIST, myelodysplastic/myeloproliferative diseases with PDGFR gene-rearrangements, and as a second-line treatment for acute lymphoblastic leukemia and aggressive systemic mastocytosis without the D816V Kit mutation (Table 4). The Kit exon 11 V560G occurs in GIST and aggressive systemic mastocytosis; Frost et al. demonstrated that this mutation has the beneficial effect of increasing the potency of imatinib by 10-fold when compared with the wild type enzyme that was expressed in murine FDC-P1 cells [89]. The auto-inhibitory JM segment interferes with imatinib binding and the V560G mutation destabilizes the dormant state and allows the drug to bind. The lesser sensitivity of the wild type enzyme should minimize adverse effects as a result of decreased inhibition of normal Kit in non-neoplastic cells. Imatinib is FDA approved for the treatment of more diseases than any other targeted small molecule protein kinase inhibitor (www.brimr.org/PKI/PKIs.htm) and it may be thought of as a broad-spectrum antagonist. This medication was initially developed to target BCR-Abl, which is the driver mutation responsible for the pathogenesis of chronic myelogenous leukemia [90]. This leukemia is characterized by the activation of Abl kinase following the translocation of its gene to the breakpoint cluster region (BCR) with the concomitant formation of the Philadelphia chromosome (Ph) that encodes a constitutively active BCR-Abl protein kinase chimera [91]. The blockade of a single enzyme by imatinib and by second- and third-generation inhibitors such as dasatinib, nilotinib, and ponatinib is thus efficacious in the treatment of this illness.

Cancers other than chronic myelogenous leukemia arise from the dysregulation of many signaling pathways [2]. The remarkable success in the treatment of this leukemia by an inhibitor of the BCR-Abl kinase is due to the unique pathogenesis involving a single biochemical defect. It is notable that this distinctive characteristic is absent from nearly all other forms of malignancy and the development of inhibitors to single targets is generally less effective in treating other neoplasms. Imatinib was the first FDA-approved orally effective targeted protein kinase inhibitor (2001) and its initial success stimulated the development and approval of an additional 36 small molecule inhibitors that interact directly with the protein kinase domain (www.brimr.org/PKI/PKIs.htm) [2]. Imatinib is also known as STI-571 (Signal Transduction Inhibitor-571), CGP 57148, Gleevec (in the United States), and Glivec (in Europe).

The X-ray structure (PDB ID: 1T46) shows that the *N*1 nitrogen of the pyridine group of imatinib forms a hydrogen bond with the N—H group of C673 (the third hinge residue) and the amino group of the tolyl-aminopyrimidine group forms a hydrogen bond with the —OH group of T670 (Sh2), the gatekeeper residue. Because the drug is bound to the DFG-D_{out} conformation, this arrangement allows a hydrogen bond to form between the αC-E640 side chain and the amide N—H and another is formed between the N—H group of DFG-D810 and the amide carbonyl oxygen of the antagonist [82]. Moreover, the piperazinyl amine forms bidentate ionic interactions with H790 (RS1) and I789 (Fig. 8B). The phenyl ring of imatinib packs loosely between the aliphatic portions of the side chains of DFG-D810, αC-E640 and L644, whereas the piperazine ring of the inhibitor makes no specific interactions with the protein but rests in a shallow pocket bounded by V643 of the αC-helix, C788 and I789 before the catalytic loop, and the catalytic loop ^{790}HRD^{792}. Overall, the drug makes hydrophobic contacts with the β1-strand L595 before the G-rich loop, V603 at the beginning of the β2-strand, the β3 A621 (CS8), V622, and K623, V643 and L644 (RS3) within the αC-helix, V654 (Sh1) within the αC-β4 back loop, V668 in the β5-strand, Y672 (the second hinge residue), C788, I789

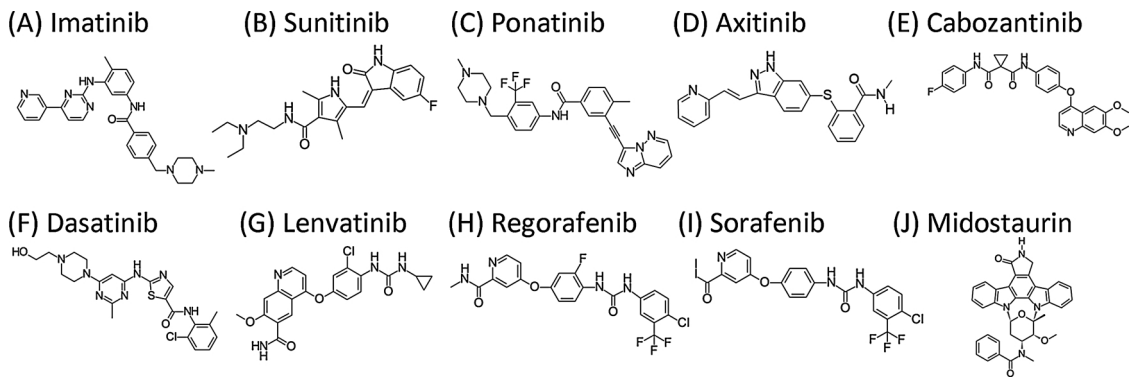

Fig. 9. Structures of selected Kit receptor multikinase inhibitors.

before the catalytic loop, R791 within the catalytic loop, L799 (CS6), C809 immediately before the activation segment, and DFG-F811 (RS2). The interaction of imatinib with residues that make up the shell residues and the catalytic and regulatory spines is illustrated in Fig. 8C and D. Imatinib occurs within the front pocket, the gate area, and BP-I-A, BP-I-B, BP-II-out, and BP-IV within the back pocket. The tolyl group occupies the back cleft hydrophobic BP-II-out pocket and the distal piperazinylphenyl group binds to BP-IV that occurs in the DFG-D_{out} configuration. Imatinib extends past the gate area in the DFG-D_{out} conformation and is therefore classified as a type IIA inhibitor. The polar contacts and hydrophobic interactions of imatinib with (i) Abl (a non-receptor protein-tyrosine kinase, PDB ID: 1IEP), (ii) colony stimulating factor-1 receptor protein-tyrosine kinase (PDB ID: 4R7I), and (iii) and PDGFRα [23] are similar.

van Linden et al. compiled a comprehensive summary of ligand and drug binding to more than 1200 human and mouse protein kinase catalytic domains [88]. Their KLIFS (kinase–ligand interaction fingerprint and structure) catalog includes an alignment of 85 ligand-binding-site residues occurring in both the small and large lobes; this listing facilitates the classification of ligands based upon their binding characteristics and expedites the detection of related interactions. Furthermore, these investigators formulated a standard amino acid residue numbering scheme that facilitates a comparison among all protein kinases. See Table 3 for the relationship between the KLIFS database numbering and the C-spine, Shell, and R-spine amino acid residue nomenclature. Of general importance, this group established an invaluable free and searchable web site that is frequently updated and provides comprehensive information on protein kinase-ligand interactions (klifs.vu-compmedchem.nl/)

Sunitinib (*N*-[2-(diethylamino)ethyl]-5-[(*Z*)-(5-fluoro-2-oxo-1H-indol-3-ylidene)methyl]-2,4-dimethyl-1H-pyrrole-3-carboxamide) (Fig. 9B) is a Kit receptor multikinase inhibitor that is FDA-approved for the first-line treatment of renal cell carcinoma and pancreatic neuroendocrine tumors and the second-line treatment of GIST (after imatinib). The drug is a potent inhibitor of the *KIT* double mutant bearing the activating (V599D) and secondary-resistance (T760I) mutations [92]. This medication was developed as an anti-angiogenesis drug and inhibits Kit, PDGF and VEGF receptors, and Flt3 (Table 4) [26,91,93]. Sunitinib is an effective inhibitor of almost all primary exon 9 extracellular segment and exon 11 JM segment mutations [78]. This agent is also an effective antagonist of enzymes bearing both exon 11 V559D primary and exon 13 V654 secondary mutations. It is less effective against Kit with exon 17 activation segment mutations. Tumors bearing extracellular exon 9 mutations are somewhat more sensitive to sunitinib than tumors with the exon 11 JM mutations and patients with exon 9 mutations have a higher response rate and longer median progression-free survival and overall survival [94].

The X-ray structure of sunitinib bound to Kit (PDB ID:3G0E) shows that the N—H of its indole group amide forms a hydrogen bond with the carbonyl group of E671 (the first hinge residue) and the drug amide N—H group forms a hydrogen bond with the carbonyl group of C673 (the third hinge residue) (Fig. 10A). This interaction mimics the binding of the adenine base of ATP with protein kinases. The antagonist also interacts hydrophobically with residues near the ceiling of the adenine pocket including L595 at the end of the β1-strand, V603 at the beginning of the β2-strand, and A621 (CS8) within the β3-strand. The antagonist makes similar contacts with V654 (Sh1) in the back loop, Y672 within the hinge, L799 (CS6) within the β7-strand, and C809, DFG-D810, DFG-F811(RS2), and activation segment A814. The diethylaminoethyl group, which extends into the solvent, is disordered and not observed. The drug interacts with the front pocket and BP-I-B of the back pocket. Sunitinib binds to the DFG-D_{out} conformation and does not extend past the gate area and is thereby classified as a type IIB inhibitor of Kit [71].

Ponatinib (3-(2-imidazo[1,2-*b*]pyridazin-3-ylethynyl)-4-methyl-*N*-[4-[(4-methylpiperazin-1-yl)methyl]-3-(trifluoromethyl)phenyl]benzamide) (Fig. 9C) is a Kit receptor multikinase inhibitor that is approved for the treatment of Ph^+ acute lymphoblastic and chronic myelogenous leukemias (www.brimr.org/PKI/PKIs.htm) and is undergoing clinical trials for the treatment of GIST, other solid tumors, and hematologic neoplasms (clinicaltrials.gov). The medication is a second generation BCR-Abl inhibitor that is effective against the Abl T315I gatekeeper mutant [95] (Table 4). Ponatinib is an effective inhibitor of the exon 11 JM segment V559D and V560G mutants as well as the T670I gatekeeper mutant [78]. It is also an effective antagonist of the activation segment D816H, D820E, and A829P mutants.

The X-ray structure of ponatinib bound to Kit (PDB ID: 4U0I) shows that the antagonist makes five hydrogen bonds with Kit. The *N*1 of the imidazopyridazine ring bonds with the carbonyl group of C673 (the third hinge residue), the N—H of the drug amino group forms a hydrogen bond with αC-E640, the benzamide carbonyl forms a hydrogen bond with the N—H group of DFG-D810, and the piperazine N—H group forms bidentate hydrogen bonds with the carbonyl groups of I789 and H790 (RS1) (Fig. 10B). Ponatinib interacts hydrophobically with residues near the ceiling of the adenine pocket including L595 at the end of the β1-strand, V603 near the beginning of the β2-strand, and the β3 A621 (CS8), V622, and K623. The antagonist makes similar contacts with L644 (RS3) and L647 within the αC-helix, I653 and V654 (Sh1) in the back loop, V688 and T670 (Sh2) in the β5-strand, and Y672 (the second hinge residue). The linear triple bond allows ponatinib to extend past the gatekeeper T670 into the back pocket and its interaction with isoleucine in the secondary imatinib-resistant T670I mutant explains its effectiveness in blocking this enzyme form. Ponatinib makes hydrophobic contact with C788, I789, H790 (RS1), and R791 within the catalytic loop. The antagonist also makes hydrophobic contact with L799 (CS8), I808, C809, and DFG-F811 (RS2). The drug binds to the front pocket, gate area, and back pockets including the BP-I-A, BP-I-B, BP-II-out, BP-III, and BP-IV subpockets (Fig. 7). This structural data indicates that ponatinib binds to the DFG-D_{out} conformation extending into the back pocket of Kit and is thereby classified as a type IIA

Table 4
Selected properties of Kit multikinase inhibitors.

Name, code, trade name*	Selected targets	Type[a]	PubChem CID[b]	Formula	MW (Da)	D/A[c]	RB[d]	FDA-approved indications (year of initial approval)[e]
Imatinib, CGP 57148, STI571, Gleevec*	BCR-Abl, Kit, PDGFRα/β,	IIA	5291	$C_{29}H_{31}N_7O$	494	2/7	7	Ph^+ CML or ALL, aggressive systemic mastocytosis, CEL, DFSP, HES, GIST, MDS/MPD (2001)
Sunitinib, SU-11248, Sutent*	VEGFR1/2/3, PDGFRα/β, Kit, Flt3, CSF-1R, RET	IIB	5329102	$C_{22}H_{27}FN_4O_2$	398	3/4	7	RCC, GIST, pNET (2006)
Ponatinib, AP24534, Iclusig*	BCR-Abl, BCR-Abl T315I, VEGFR, FGFR, EphR, Src family kinases, Kit, PDGFRα/β, RET, Tie2, Flt3	IIA	24826799	$C_{29}H_{27}F_3N_6O$	533	1/8	6	Ph^+ CML, ALL (2012)
Axitinib, AG-013736, Inlyta*	VEGFR1/2/3, PDGFRβ, Kit	IIA	6450551	$C_{22}H_{18}N_4OS$	386	2/4	5	RCC (2012)
Cabozantinib, XL184, Cometriq	VEGFR1/2/3, RET, Met, Kit, TrkB, Flt3, Axl, Tie2, ROS1	IIA	25102847	$C_{28}H_{24}FN_3O_5$	502	2/7	8	Advanced medullary thyroid cancer (2012), RCC (2016)
Dasatinib, BMS-354825, Sprycel*	BCR-Abl, Src, Lck, Yes, Fyn, Kit, EphA2, PDGFRα/β,	IIB	3062316	$C_{22}H_{26}ClN_7O_2S$	488	3/9	7	Ph^+ CML, ALL (2006)
Lenvatinib, E7080, AK175809, Lenvima*	VEGFRs, PDGFRα/β, FGFRs, Kit, RET	IIA	9823820	$C_{21}H_{19}ClN_4O_4$	427	3/5	6	Differentiated thyroid cancer (2015)
Regorafenib, BAY 73–4506, Stivarga*	VEGFR1/2/3, BCR-Abl, Raf, B-Raf V600E, Kit, PDGFRα/β, RET, FGFR1/2, Tie2, Eph2A	IIA	11167602	$C_{21}H_{15}ClF_4N_4O_3$	483	3/8	5	CRC, GIST (2012)
Sorafenib, BAY 43–9006, Nexavar*	B/C-Raf, B-Raf (V600E), PDGFRα/β, Kit, Flt3, RET, VEGFR1/2/3	IIA	216239	$C_{21}H_{16}ClF_3N_4O_3$	465	3/7	5	Hepatocellular carcinoma, RCC, differentiated thyroid cancer (2005)
Midostaurin, PKC412, Rydapt*	Flt3, Kit, Kit D816V, PDGFRα/β, VEGFR2, PKC	I	9829523	$C_{35}H_{30}N_4O_4$	571	1/4	3	AML Flt3-mutation positive, aggressive systemic mastocytosis, MCL (2017)

[a] Type of inhibitor based upon the drug-kinase structure.

[b] pubchem.ncbi.nlm.nih.gov.

[c] D, no. of hydrogen bond donors; A, no. of hydrogen bond acceptors.

[d] No. of rotatable bonds.

[e] ALL, acute lymphoblastic leukemia; AML, acute myelogenous leukemia; CEL, chronic eosinophilic leukemia; CML, chronic myelogenous leukemia; CRC, colorectal cancer; DFSP, dermatofibrosarcoma protuberans; GIST, gastrointestinal stromal tumor; HES, hypereosinophilic syndrome; MCL, mast cell leukemia; MDS/MPD, myelodysplastic/myeloproliferative diseases; Ph^+, Philadelphia chromosome positive; pNET, pancreatic neuroendocrine tumor; RCC, renal cell carcinoma.

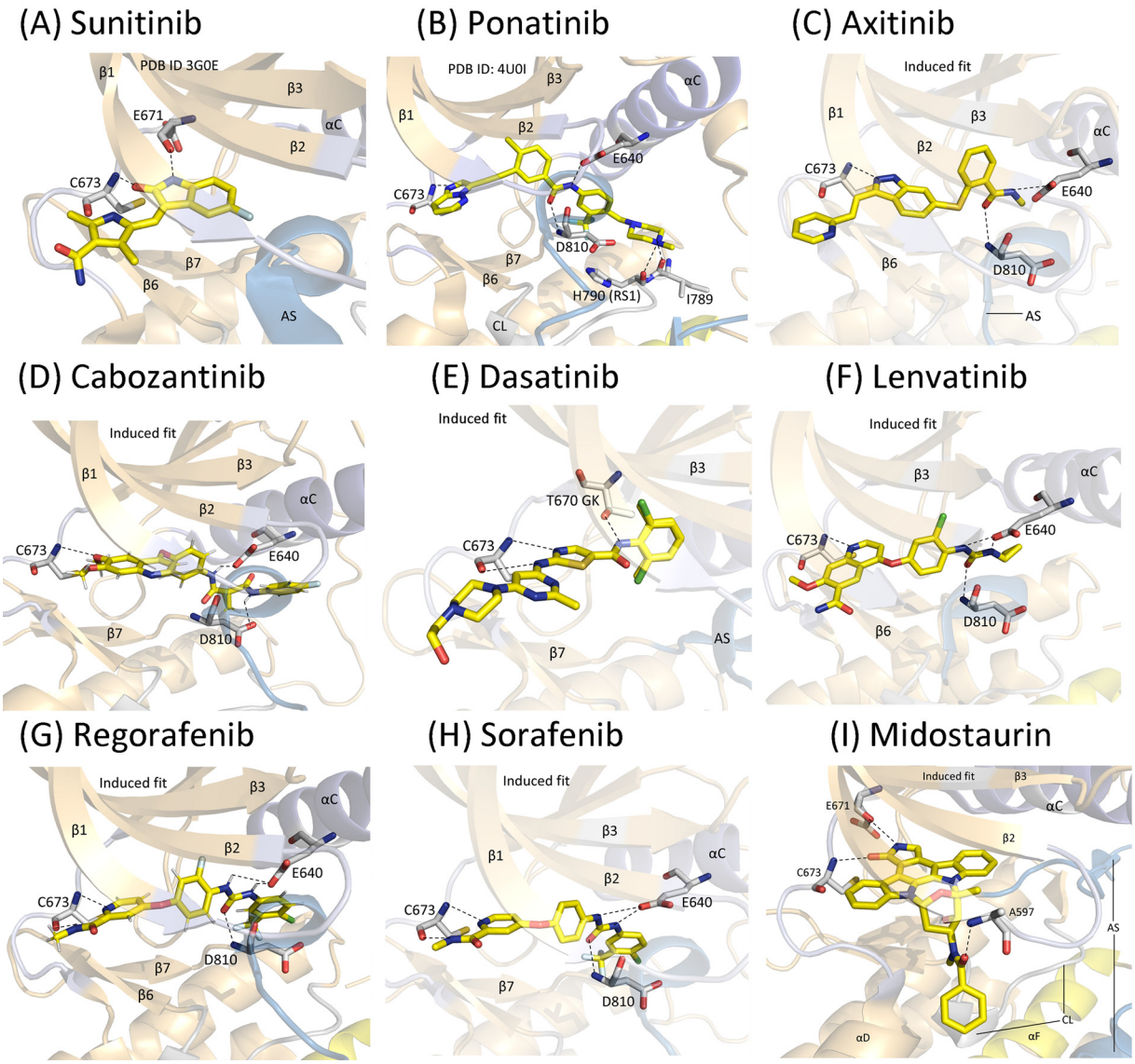

Fig. 10. Structures of Kit-drug complexes. The carbon atoms of the drugs are colored yellow. AS, activation segment; CL, catalytic loop; GK, gatekeeper. The dashed lines depict polar bonds.

inhibitor [71]. The Schrödinger induced fit computer-generated structure of ponatinib binding to PDGFRα [23] closely resembles the X-ray structure of its binding to Kit described here.

Axitinib (*N*-Methyl-2-((3-(2-(pyridin-2-yl)vinyl)-1H-indazol-6-yl) thio)benzamide) (Fig. 9D) is an orally effective second generation Kit, PDGFRα/β and VEGFR1/2/3 antagonist that was FDA approved as a second-line treatment for renal cell carcinomas in 2012. Both PDGF and VEGF receptors participate in angiogenesis and the observed therapeutic response may be related to the inhibition of both of these families of enzymes [95–97]. Whether Kit inhibition plays a therapeutic effect against renal cell carcinoma is unclear. Although there are no structural data of axitinib bound to Kit, we were able to produce a satisfactory pose of the ligand binding to human Kit using the Schrödinger induced fit docking protocol (2016-1 release) [98] with 1T46 (PDB: ID) as a template. Using the terminology of Fresner et al., pose refers to the description of the orientation and position of the ligand relative to its target [99]. The resulting computer-generated structure indicates that the indazole *N*2 forms a hydrogen bond with the N—H group of C673 (the third hinge residue). The benzamide carbonyl group hydrogen bonds with the N—H group of DFG-D810 and the benzamide N—H group forms a hydrogen bond with αC-E640 (Fig. 10C). The drug interacts hydrophobically with residues near the ceiling of the adenine pocket including L595 within the β1-strand, V603 within the β2-strand, and A621 (CS8) and K623 within the β3-strand. Axitinib also interacts hydrophobically with αC-L644 (RS3), V654 (Sh1) within the αC-β4 back loop, V668 in the β5-strand, Y672 within the hinge, L799 (CS6) within the β7-strand on the floor of the adenine binding pocket, C809 before the activation segment, and DFG-F811 (RS2). The pyridine ring of axitinib is directed away from the enzyme into the solvent. The drug binds in the front pocket, gate area, and back pockets including the BP-I-A, BP-I-B, and BP-II-out; in contrast to imatinib and ponatinib, axitinib does not extend into the BP-IV subpocket. This structural data indicates that ponatinib binds to the DFG-D_{out} conformation extending into the back pocket of Kit and is thereby classified as a type IIA inhibitor [71].

Cabozantinib (1-*N*-[4-(6,7-dimethoxyquinolin-4-yl) oxyphenyl]-1-*N*′-(4-fluorophenyl) cyclopropane-1,1-dicarboxamide) is a multikinase inhibitor [100] that is FDA approved for the first-line treatment of advanced (i) medullary thyroid cancer and (ii) renal cell carcinoma (Table 4) [101]. Although there are no structural data of cabozantinib (Fig. 9E) binding to Kit or any other protein kinase in the public domain, we were able to generate a satisfactory pose of the drug binding to human Kit using the Schrödinger induced fit docking protocol as

described above using PDB ID: 1T46 as a template [98]. The resulting pose indicates that the cabozantinib quinoline *N*1 forms a hydrogen bond with the N−H group of C793 of the hinge and one amide group forms a hydrogen bond with αC-E640 and the second amide forms a hydrogen bond with the D810 carboxylate group (Fig. 10D). The antagonist makes hydrophobic interactions with L595 at the end of the β1-strand, V603 at the beginning of the β2-strand, A621 (CS8) and K623 within the β3-strand, and A636, V643, L644 (RS3), and L645 within the αC-helix. The drug also makes hydrophobic contacts with V654 (Sh1) of the αC-β4 back loop, Y672 (the second hinge residue), L799 (CS6) on the floor of the adenine pocket, C809 before the activation segment, and F811 (RS2) and A814 within the activation segment. The antagonist also makes van der Waals contact with the Sh2 gatekeeper (T670) and D810 (RS2). Cabozantinib binds in the front pocket, gate area, and back pockets including the BP-I-A, BP-I-B, BP-II-out, BP-III, and BP-IV subpockets. The compound binds to an inactive DFG-D_{out} conformation of Kit and extends into the back pocket is thereby classified as a type IIA inhibitor [71].

Dasatinib (*N*-(2-chloro-6-methylphenyl)-2-[[6-[4-(2-hydroxyethyl) piperazin-1-yl]-2-methylpyrimidin-4-yl]amino]-1,3-thiazole-5-carboxamide) (Fig. 9F) was initially developed as a BCR-Abl inhibitor and was subsequently shown to inhibit Kit, PDGFR, and Src family kinases including Src, Lck, and Yes [102–106]. Inhibition of BCR-Abl is clinically effective and led to the FDA-approval for the treatment of Ph^+ chronic myelogenous leukemia and acute lymphoblastic leukemia. Kit, PDGFR, and Src family kinases participate in a variety of signaling pathways that promote cell proliferation and survival and possible dasatinib therapeutic responses in patients with mastocytosis, melanomas, other solid tumors, and hematopoietic disorders may be related to the inhibition of these enzymes [102,103,107]. Because Src family kinases are important mediators of Kit signaling, dual inhibition of Kit and Src kinases may be responsible for its clinical efficacy [108]. This agent is effective against the *KIT* D816 V mutant (IC_{50} value of 32 nM) when comparted with imatinib (no inhibition at 10 μM) [103]. Dasatinib is FDA-approved for the first- or second-line treatment of Ph^+ chronic myelogenous leukemia or the second-line treatment of Ph^+ acute lymphoblastic leukemias (Table 4).

No X-ray structural studies of dasatinib bound to Kit have been reported, but we were able to generate a reasonable pose of the drug binding to the human receptor with the Schrödinger induced fit docking protocol [98] as described above. The best pose shows that the *N*3 of the thiazole forms a hydrogen bond with the N−H group of C673 while the adjacent dasatinib amino group forms a hydrogen bond with the carbonyl group of C673 (the third hinge residue). Moreover, the carboxamide *N*−H forms a hydrogen bond with the −OH group of the T670 gatekeeper residue (Fig. 10E). The antagonist interacts hydrophobically with residues near the top of the adenine pocket including L595 at the end of the β1-strand, V603 of the β2-strand, and A621 (CS8), V622, and K623 within the β3-strand. Dasatinib also makes hydrophobic contact with V654 (Sh1) and L657 of the back loop, with V668 and I669 of the β5-strand, and Y672 of the hinge. It also interacts hydrophobically with L799 (CS6) of the β7-strand along with C809, which precedes DFG-D810 of the activation segment, and with DFG-F811.The 2-hydroxyethylpiperazine group extends into the solvent. The drug binds in the front pocket and the gate area. Dasatinib interacts with the DFG-D_{out} conformation of Kit and does not extend past the gate area and is classified as a type IIB inhibitor [71].

Lenvatinib (4-[3-chloro-4-(cyclopropylcarbamoylamino)phenoxy]-7-methoxyquinoline-6-carboxamide) (Fig. 9G) is a Kit multikinase antagonist that is FDA approved for the second-line treatment of differentiated follicular and papillary thyroid cancers that are insensitive to radioiodine treatment (Table 4). This medication was initially developed as an angiogenesis inhibitor with activity against VEGFR, PDGFR, and Kit [109]. We used the Schrödinger induced fit protocol [98] to dock the ligand into human Kit as described above. The pose shows that *N*1 of the quinoline moiety forms a hydrogen bond with the N−H group of the third hinge residue (C673), each of the two ureido N−H groups forms a hydrogen bond with αC-E640, the carbonyl oxygen of the ureido group forms a hydrogen bond with the N−H group of DFG-D810 (Fig. 10F). Lenvatinib interacts hydrophobically with several residues of Kit; these residues include L595 at the end of the β1-strand, V603 near the beginning of the β2-strand, the β3-strand A621 (CS8) and K623, which make up the roof of the adenine binding pocket. The drug also interacts hydrophobically with L644 (RS3) within the αC-helix and Y672 (the second hinge residue). Moreover, the antagonist makes similar contacts with L799 (CS6) in the β7-strand, C809 immediately before the activation segment, and DFG-F811 (RS2). The 7-methoxy group extends into the solvent. The antagonist binds in the front pocket, gate area, and back pockets including BP-I-A, BP-I-B, and BP-II-out; unlike imatinib and ponatinib, lenvatinib does not extend into the BP-IV subpocket. The drug extends into the back pocket of the DFG-D_{out} conformation of Kit and is classified as a type IIA inhibitor [71].

Regorafenib (4-[4-[[4-chloro-3-(trifluoromethyl)phenyl]carbamoylamino]-3-fluorophenoxy]-N-methylpyridine-2-carboxamide) (Fig. 9H) is a Kit multikinase inhibitor that is an FDA-approved second-line treatment of hepatocellular carcinoma following sorafenib treatment, third-line treatment of GIST following imatinib and sunitinib, and third- or fourth-line treatment of advanced colorectal cancer (Table 4). Like lenvatinib, the medication was initially developed as an angiogenesis inhibitor with activity against receptor protein-tyrosine kinases including VEGFR1/2, PDGFRβ, Kit, and RET as well as the protein-serine/threonine kinase B-Raf [110]. We used the Schrödinger Glide protocol [98] to dock the drug into human Kit as described above. The pose shows that the pyridine *N* forms a hydrogen bond with the N−H group of C673 and carbamoyl amino group forms a hydrogen bond with the carbonyl group of C673 (the third hinge residue). The ureido carbonyl group forms a hydrogen bond with the N−H group of DFG-D810 and the ureido nitrogen atoms form hydrogen bonds with the αC-E640 (Fig. 10G). Regorafenib makes hydrophobic contact with L595 at the end of the β1-strand, V603 at the beginning of the β2-strand, A621 (CS8) and K623 in the β3-strand that together form the roof of the adenine binding pocket. The antagonist makes further hydrophobic contacts with αC V643, L644 (RS3), and L647 along with I653 and V654 (Sh1) of the αC-β4 back loop. It also makes hydrophobic contact with Y672 (the second hinge residue), L783, C788, H790 (RS1), and L799 (CS6) on the floor of the adenine binding pocket. The medication makes additional hydrophobic contact with I808 and L809 preceding the activation segment as well as DFG-F811 (RS2). Regorafenib differs from sorafenib, described next, by the addition a fluorine atom to the phenoxy group. This fluorine atom is sandwiched between K623 and the T670 gatekeeper (Sh2). The drug binds in the front pocket, gate area, BP-I-B, BP-II-out, and BP-III back subpockets as illustrated in Fig. 7. The 7-methoxy group extends into the solvent. The hydrogen bonds with a hinge residue, the αC-E, and DFG-D_{out} are characteristic of classical type IIA inhibitors [82]. As a type IIA inhibitor, it is not surprising that this antagonist is not a good inhibitor of the exon 17 activation segment D816H mutation [78].

Sorafenib (4-[4-[[4-chloro-3-(trifluoromethyl)phenyl]carbamoylamino]phenoxy]-*N*-methylpyridine-2-carboxamide) (Fig. 9I) is a Kit receptor multikinase inhibitor that is FDA-approved for the first-line treatment of hepatocellular and renal cell carcinomas and as a second-line treatment of radioiodine-refractory differentiated follicular and papillary thyroid carcinomas (www.brimr.org/PKI/PKIs.htm). This medication was initially developed as a Raf protein-serine/threonine kinase inhibitor, but it is a potent antagonist of several receptor protein kinases as well (Table 4) [111–113]. We used the Schrödinger induced fit docking protocol [98] to generate a model for the interaction of this ligand with Kit as described above. The resulting pose shows that the antagonist makes five hydrogen bonds with Kit. The terminal carboxamide N−H forms a hydrogen bond with the carbonyl group of C673 and the *N*1 of the pyrimidine forms a hydrogen bond with the N−H group of C673 (the third hinge residue). The two ureido N−H groups

form hydrogen bonds with the carboxyl group of αC-E640 and the ureido carbonyl group forms a hydrogen bond with the N—H group of DFG-D810 (Fig. 10H). Moreover, the drug interacts hydrophobically with residues near the ceiling of the adenine pocket including L595 at the end of the β1-strand, V603 near the beginning of the β2-strand, and the β3-strand A621 (CS8). It makes similar contacts with L644 (RS3) and L647 of the αC-helix, I651 and V654 (Sh1) in the αC-β4 back loop, and Y672 (the second hinge residue). Sorafenib also makes hydrophobic contact with L783, H790 (RS1), L799 (CS6) on the floor of the adenine pocket along with I808 and C809 preceding the activation segment. Sorafenib binds in the front pocket, the gate area, and BP-I-B, BP-II-out, and BP-III in the back pocket. Like several of the previous drugs, sorafenib extends into the back pocket of the DFG-D_{out} conformation of Kit and is thereby classified as a type IIA inhibitor [71]. Sorafenib and regorafenib are congeners developed by Bayer. Owing to the FDA-approval of regorafenib for the treatment of GIST, it is unclear whether Bayer will continue to develop sorafenib for the treatment of GIST [31].

Midostaurin (*N*-((9S,10R,11R,13R)-10-methoxy-9-methyl-1-oxo-2,3,10,11,12,13-hexahydro-9,13-epoxy-1H,9H-diindolo(1,2,3-GH:3',2',1'-lm)pyrrolo(3,4-j)(1,7)benzodiazonin-11-yl)-n-methylbenzamide) (Fig. 9J) is a Kit multikinase inhibitor that is FDA-approved as a first-line treatment for (i) aggressive systemic mastocytosis, (ii) systemic mastocytosis with associated hematologic neoplasm, (iii) mast cell leukemia, and (iv) as a combination treatment of acute myelogenous leukemia with $Flt3^+$ mutations [32,114,115]. This drug was initially developed as a PKC protein-serine/threonine kinase inhibitor, but it is a potent antagonist of several receptor protein kinases as well (Table 4). Midostaurin is a derivative of staurosporine, which is a bacterially (*Streptomyces stauroporeus*) produced alkaloid that inhibits a large number of protein kinases (a pan-protein kinase inhibitor). Importantly, this antagonist is effective against Kit exon 17 activation segment D816 V/Y mutations [116]. Midostaurin is currently in clinical trials for patients with systemic mastocytosis, mast cell leukemia, *KIT* mutant acute myelogenous leukemia, and other hematologic disorders (www.clinicaltrials.gov).

We used the Schrödinger induced fit docking protocol [98] to generate a model for the interaction of midostaurin with the active form of Kit using PDB ID: 1PKG as a template. The resulting pose shows that the antagonist makes three hydrogen bonds with Kit. The *N*1 pyrrolo N—H forms a hydrogen bond with the carbonyl group of E671, the pyrrolo carbonyl group forms a hydrogen bond with C673 N—H group of C673 (the third hinge residue), and the benzamide carbonyl forms a hydrogen bond with the A597 N—H group (the second residue of the G-rich loop) (Fig. 10I). Moreover, the drug interacts hydrophobically with residues near the ceiling of the adenine pocket including L595 at the end of the β1-strand, V603 near the beginning of the β2-strand, the β3-strand A621 (CS8) and K623, and with Y672 (the second hinge residue). Midostaurin also makes hydrophobic contact with L679 and N880, which link the hinge to the αD-helix, R796 near the end of the catalytic loop, L799 (CS6), and C809 that occurs before DFG-D810 of the activation segment. Midostaurin binds in the front pocket including FP-II and it does not extend into the gate area. Unlike the previous drugs, midostaurin binds to the active enzyme and is classified as a type I inhibitor [71].

To summarize this section, the ten drugs form a hydrogen bond with C673 (the third hinge residue) and they interact hydrophobically with β1-strand L595, the β2-strand V603, A621 (CS8), Y672 (the second hinge residue), L799 (CS6) on the floor of the adenine pocket, and C809 immediately before the activation segment. All of the drugs except dasatinib and midostaurin interact hydrophobically with V654 (Sh1) within the back loop. All of the antagonists except for axitinib, dasatinib, midostaurin, and sorafenib make hydrophobic interactions with K623 within the β3-strand AxK signature. Imatinib, sunitinib, axitinib, lenvatinib, regorafenib, and sorafenib form hydrogen bonds with C673 of the hinge, E640 of the αC-helix, and the N—H group of D810; this is a classical type II drug-enzyme interaction [82]. Pazopanib is a Kit multikinase inhibitor that is FDA-approved for the treatment of renal cell carcinomas and soft tissue sarcomas. We were unable to obtain any satisfactory poses of this ligand bound to Kit using the Schrödinger Induced Fit or Glide programs [98,99].

5. Epilogue

Imatinib (Gleevec) is an FDA-approved treatment for advanced GIST (www.brimr.org/PKI/PKIs.htm); however, resistance generally develops in a median time of two years owing to secondary-resistance mutations in *KIT*. Sunitinib and regorafenib are FDA approved as second- and third-line therapies for these patients. When resistance to all three agents occurs such patients lack additional effective and approved treatment options. Several alternative medications such as alvocidib, amcasertib, avapritinib, axitinib, BYL719 (a phosphatidylinositol 3′-phosphate kinase inhibitor), dovitinib, ganetespib and onalespib (heat shock protein chaperone inhibitors), cabozantinib, crenolanib, linsitinib, masitinib, OSI-930, nilotinib, pexidartinib, ponatinib, semaxanib, vandetanib, and sorafenib are being evaluated along with immunotherapies, radiation, and traditional cytotoxic drugs (www.clinicaltrials.gov). So-called liquid biopsies that permit the analysis of circulating tumor DNA (ctDNA) for resistance mutations, which allows for early switches to alternative therapy, may prove beneficial. Additional strategies for the treatment of tumors bearing secondary-resistance mutation include the use of a combination of agents that target (i) two different proteins in the same pathway or (ii) two different signaling pathways. Another possibility is to combine targeted agents with cytotoxic drugs. See Ref. [26] for a complete discussion of additional targets, therapies, and clinical trials for the treatment of GIST.

Although the pose or mode of binding of each ligand with its protein kinase target is unique, it is advantageous to classify drug-enzyme interactions and use them in the drug discovery process. We have classified protein kinase inhibitors into seven possible types (I–VI and I½) based upon the structures of the drug-protein kinase complexes [71]. Because some medicinals are able to bind to multiple conformations of their protein kinase targets the complexity of inhibitor taxonomy increases. For example, bosutinib is a type I antagonist of Src and a type IIB antagonist of the Abl (both are non-receptor protein-tyrosine kinases). Crizotinib is a type I inhibitor of the ALK and a type I½B inhibitor of c-Met (both are receptor protein-tyrosine kinases). Sunitinib is a type I½B inhibitor of CDK2 (cyclin-dependent protein kinase 2, a protein-serine/threonine kinase) and a type IIB inhibitor of Kit (a receptor protein-tyrosine kinase) [8,15]. Adding to this complexity, X-ray crystallographic structures indicate that erlotinib can be a type I or I½B inhibitor of EGFR/ErbB1 (a receptor protein-tyrosine kinase). These results indicate that some protein kinase antagonists lack conformational selectivity. Moreover, imatinib, the prototypical type II inhibitor, was observed to bind to the active non-receptor Syk protein-tyrosine kinase with αC_{in} and an open DFG-D_{in} activation segment conformation as a type I inhibitor (PDB ID: 1XBB) [117]. In contrast to its binding to Kit in an extended linear conformation (Fig. 10), imatinib assumes a compact U-shaped structure that occurs only within the front pocket.

Although targeted protein kinase inhibitors generally produce less severe adverse events when compared with cytotoxic drugs, nevertheless side effects are commonly observed. For example, multikinase inhibitors that block VEGFR signaling usually produce hypertension [118]. Although Kit expression is low in most adult cells, nevertheless various stem cells produce Kit receptors and SCF. Moreover, Kit inhibition has been associated with cardiac toxicity. In an experimental study, Savi et al. found that imatinib induced human cardiac progenitor cell depletion, reduced growth, and increased cell death in cell culture, an effect that was attributed to Kit inhibition [119]. See Ref. [120] for a review of Kit function in the developing and adult heart.

As indicated in Table 4, all of the drugs reviewed in this paper target

several enzymes. There are more than 175 different orally effective protein kinase inhibitors in clinical trials worldwide [121]; a complete listing can be found at www.icoa.fr/pkidb/. Although one goal in drug discovery and development of protein kinase antagonists has been to inhibit a single enzyme, it appears that many, if not most, of so-called selective inhibitors have been found at later stages to inhibit multiple enzymes. It appears that the vast majority of FDA-approved protein kinase antagonists are multikinase inhibitors (www.brimr.org/PKI/PKIs.htm). Their therapeutic success and perhaps toxicity may be related to the simultaneous inhibition of multiple enzymes. Accordingly, we have the question of whether magic shotguns are to be favored over magic bullets [122].

Manning et al. established that the human protein kinase super family consists of 518 members [4]. If the number of human genes is about 19,000 [68], then protein kinases make up 2.7% of all genes. Thus, about 1 in 37 genes encodes a protein kinase. Because mutations and dysregulation of protein kinases play fundamental roles in the pathogenesis of human diseases including autoimmune, inflammatory, and nervous disorders as well as cancer, this family of enzymes has become one of the most important drug targets over the past two decades [1,2]. There are about three dozen FDA-approved medications that are directed against about 20 different protein kinases (www.brimr.org/PKI/PKIs.htm) and drugs targeting an additional 20 protein kinases are in clinical trials worldwide [3]. Owing to the hundreds of disease loci or cancer amplicons that have been mapped in the human genome [4], one can anticipate a substantial increase in the number of enzymes that will be targeted for the treatment of more and more illnesses.

Conflict of interest

The author is unaware of any affiliations, memberships, or financial holdings that might be perceived as affecting the objectivity of this review.

Acknowledgment

The colored figures in this paper were checked to ensure that their perception was accurately conveyed to colorblind readers [123]. The author thanks Laura M. Roskoski for providing editorial and bibliographic assistance. I also thank Josie Rudnicki and Jasper Martinsek for their help in preparing the figures and Pasha Brezina and W.S. Sheppard for their help in structural analyses.

References

[1] P. Cohen, Protein kinases – the major drug targets of the twenty-first century? Nat. Rev. Drug Discov. 1 (2002) 309–315.
[2] R. Roskoski Jr., A historical overview of protein kinases and their targeted small molecule inhibitors, Pharmacol. Res. 100 (2015) 1–23.
[3] P.M. Fischer, Approved and experimental small-molecule oncology kinase inhibitor drugs: a mid-2016 overview, Med. Res. Rev. 37 (2017) 314–367.
[4] G. Manning, D.B. Whyte, R. Martinez, T. Hunter, S. Sudarsanam, The protein kinase complement of the human genome, Science 298 (2002) 1912–1934.
[5] A. Alonso, R. Pulido, The extended human PTPome: a growing tyrosine phosphatase family, FEBS J. 283 (2016) 1404–1429 Erratum in: FEBS J 2016;283:2197–2201.
[6] P. Besmer, J.E. Murphy, P.C. George, F.H. Qiu, P.J. Bergold, L. Lederman, et al., A new acute transforming feline retrovirus and relationship of its oncogene v-*kit* with the protein kinase gene family, Nature 320 (1986) 415–421.
[7] Y. Yarden, W.J. Kuang, T. Yang-Feng, L. Coussens, S. Munemitsu, T.J. Dull, et al., Human proto-oncogene c-*kit*: a new cell surface receptor tyrosine kinase for an unidentified ligand, EMBO J. 6 (1987) 3341–3351.
[8] R. Roskoski Jr., Signaling by Kit protein-tyrosine kinase-The stem cell factor receptor, Biochem. Biophys. Res. Commun. 337 (2005) 1–13.
[9] J. Lennartsson, L. Rönnstrand, Stem cell factor receptor/c-Kit: from basic science to clinical implications, Physiol. Rev. 92 (2012) 1619–1649.
[10] S.D. Lyman, S.E. Jacobsen, c-*kit* ligand and Flt3 ligand: stem/progenitor cell factors with overlapping yet distinct activities, Blood 91 (1998) 1101–1134.
[11] B. Motro, J.M. Wojtowicz, A. Bernstein, D. van der Kooy, Steel mutant mice are deficient in hippocampal learning but not long-term potentiation, Proc. Natl. Acad. Sci. U. S. A. 5 (1996) 1808–1813.
[12] S. Lourenssen, B. Motro, A. Bernstein, J. Diamond, Defects in sensory nerve numbers and growth in mutant Kit and Steel mice, Neuroreport 11 (2000) 1159–1165.
[13] W.J. Fantl, D.E. Johnson, L.T. Williams, Signaling by receptor tyrosine kinases, Annu. Rev. Biochem 62 (1993) 453–481.
[14] M.A. Lemmon, J. Schlessinger, Cell signaling by receptor tyrosine kinases, Cell 141 (2010) 1117–1134.
[15] R. Roskoski Jr., Structure and regulation of Kit protein-tyrosine kinase-The stem cell factor receptor, Biochem. Biophys. Res. Commun. 338 (2005) 1307–1315.
[16] N. Oiso, K. Fukai, A. Kawada, T. Suzuki, Piebaldism, J. Dermatol. 40 (2013) 330–335.
[17] T. Furitsu, T. Tsujimura, T. Tono, H. Ikeda, H. Kitayama, U. Koshimizu, et al., Identification of mutations in the coding sequence of the proto-oncogene c-kit in a human mast cell leukemia cell line causing ligand-independent activation of c-kit product, J. Clin. Invest. 92 (1993) 1736–1744.
[18] N.J. Dibb, S.M. Dilworth, C.D. Mol, Switching on kinases: oncogenic activation of BRAF and the PDGFR family, Nat. Rev. Cancer 4 (2004) 718–727.
[19] C.L. Corless, C.M. Barnett, M.C. Heinrich, Gastrointestinal stromal tumours: origin and molecular oncology, Nat. Rev. Cancer 11 (2011) 865–878.
[20] H.P. Horny, K. Sotlar, P. Valent, K. Hartmann, Mastocytosis: a disease of the hematopoietic stem cell, Dtsch. Arztebl. Int. 105 (2008) 686–692.
[21] A. Orfao, A.C. Garcia-Montero, L. Sanchez, L. Escribano, Recent advances in the understanding of mastocytosis: the role of KIT mutations, Br. J. Haematol. 138 (2007) 12–30.
[22] S. Hirota, K. Isozaki, Y. Moriyama, K. Hashimoto, T. Nishida, S. Ishiguro, et al., Gain-of-function mutations of c-kit in human gastrointestinal stromal tumors, Science 279 (1998) 577–580.
[23] R. Roskoski Jr, The role of small molecule platelet-derived growth factor receptor (PDGFR) inhibitors in the treatment of neoplastic disorders, Pharmacol. Res. 129 (2018) 65–83.
[24] V.P. Balachandran, R.P. DeMatteo, Gastrointestinal stromal tumors: who should get imatinib and for how long? Adv. Surg. 48 (2014) 165–183.
[25] A. Poveda, X. García Del Muro, J.A. López-Guerrero, R. Cubedo, V. Martínez, I. Romero, et al., GEIS guidelines for gastrointestinal sarcomas (GIST), Cancer Treat. Rev. 55 (2017) 107–119.
[26] A. Wozniak, Y.K. Gebreyohannes, M. Debiec-Rychter, P. Schöffski, New targets and therapies for gastrointestinal stromal tumors, Expert Rev. Anticancer Ther. 17 (2017) 1117–1129.
[27] P.G. Casali, J. Zalcberg, A. Le Cesne, P. Reichardt, J.Y. Blay, L.H. Lindner, et al., Ten-year progression-free and overall survival in patients with unresectable or metastatic GI stromal tumors: long-term analysis of the European organisation for research and treatment of cancer, Italian sarcoma group, and Australasian gastrointestinal trials group intergroup phase iii randomized trial on imatinib at two dose levels, J. Clin. Oncol. 35 (2017) 1713–1720.
[28] G.D. Demetri, A.T. van Oosterom, C.R. Garrett, M.E. Blackstein, M.H. Shah, J. Verweij, et al., Efficacy and safety of sunitinib in patients with advanced gastrointestinal stromal tumour after failure of imatinib: a randomised controlled trial, Lancet 368 (2006) 1329–1338.
[29] G.D. Demetri, P. Reichardt, Y.K. Kang, J.Y. Blay, P. Rutkowski, H. Gelderblom, et al., Efficacy and safety of regorafenib for advanced gastrointestinal stromal tumours after failure of imatinib and sunitinib (GRID): an international, multicentre, randomised, placebo-controlled, phase 3 trial, Lancet 381 (2013) 295–302.
[30] X. Zhao, C. Yue, Gastrointestinal stromal tumor, J. Gastrointest. Oncol. 3 (2012) 189–208.
[31] C. Serrano, S. George, C. Valverde, D. Olivares, A. García-Valverde, C. Suárez, et al., Novel insights into the treatment of imatinib-resistant gastrointestinal stromal tumors, Target Oncol. 12 (2017) 277–288.
[32] J. Gotlib, H.C. Kluin-Nelemans, T.I. George, C. Akin, K. Sotlar, O. Hermine, et al., Efficacy and safety of midostaurin in advanced systemic mastocytosis, N. Engl. J. Med. 374 (2016) 2530–2541.
[33] K. Hartmann, B.M. Henz, Mastocytosis: recent advances in defining the disease, Br. J. Dermatol. 144 (2001) 682–695.
[34] M. Solh, S. Yohe, D. Weisdorf, C. Ustun, Core-binding factor acute myeloid leukemia: heterogeneity, monitoring, and therapy, Am. J. Hematol. 89 (2014) 1121–1131.
[35] R.L. Siegel, K.D. Miller, A. Jemal, Cancer statistics, 2018, CA. Cancer J. Clin. 68 (2018) 7–30.
[36] A. Najem, M. Krayem, A. Perdrix, J. Kerger, A. Awada, F. Journe, et al., New drug combination strategies in melanoma: current status and future directions, Anticancer Res. 37 (2017) 5941–5953.
[37] B.Y. Reddy, D.M. Miller, H. Tsao, Somatic driver mutations in melanoma, Cancer 123 (2017) 2104–2117.
[38] M.C. Heinrich, C.D. Blanke, B.J. Druker, C.L. Corless, Inhibition of KIT tyrosine kinase activity: a novel molecular approach to the treatment of KIT-positive malignancies, J. Clin. Oncol. 20 (2002) 1692–1703.
[39] S.K. Hanks, T. Hunter, Protein kinases 6: The eukaryotic protein kinase superfamily: kinase (catalytic) domain structure and classification, FASEB J. 9 (1995) 576–596.
[40] D.R. Knighton, J.H. Zheng, L.F. Ten Eyck, V.A. Ashford, N.H. Xuong, S.S. Taylor, et al., Crystal structure of the catalytic subunit of cyclic adenosine monophosphate-dependent protein kinase, Science 253 (1991) 407–414.
[41] D.R. Knighton, J.H. Zheng, L.F. Ten Eyck, N.H. Xuong, S.S. Taylor, J.M. Sowadski, Structure of a peptide inhibitor bound to the catalytic subunit of cyclic adenosine monophosphate-dependent protein kinase, Science 253 (1991) 414–420.
[42] R. Roskoski Jr., Src protein-tyrosine kinase structure, mechanism, and small

molecule inhibitors, Pharmacol. Res. 94 (2015) 9–25.
[43] A.C. Bastidas, M.S. Deal, J.M. Steichen, Y. Guo, J. Wu, S.S. Taylor, Phosphoryl transfer by protein kinase A is captured in a crystal lattice, J. Am. Chem. Soc. 135 (2013) 4788–4798.
[44] R.S. Vijayan, P. He, V. Modi, K.C. Duong-Ly, H. Ma, J.R. Peterson, et al., Conformational analysis of the DFG-out kinase motif and biochemical profiling of structurally validated type II inhibitors, J. Med. Chem. 58 (2015) 466–479.
[45] S.S. Taylor, M.M. Keshwani, J.M. Steichen, A.P. Kornev, Evolution of the eukaryotic protein kinases as dynamic molecular switches, Philos. Trans. R Soc. Lond. B Biol. Sci. 367 (2012) 2517–2528.
[46] B. Nolen, S. Taylor, G. Ghosh, Regulation of protein kinases; controlling activity through activation segment conformation, Mol. Cell 15 (2004) 661–675.
[47] D.J. Rawlings, A.M. Scharenberg, H. Park, M.I. Wahl, S. Lin, R.M. Kato, et al., Activation of BTK by a phosphorylation mechanism initiated by SRC family kinases, Science 271 (1996) 822–825.
[48] J.P. DiNitto, G.D. Deshmukh, Y. Zhang, S.L. Jacques, R. Coli, J.W. Worrall, et al., Function of activation loop tyrosine phosphorylation in the mechanism of c-Kit auto-activation and its implication in sunitinib resistance, J. Biochem. 147 (2010) 601–609.
[49] S. Yuzawa, Y. Opatowsky, Z. Zhang, V. Mandiyan, I. Lax, J. Schlessinger, Structural basis for activation of the receptor tyrosine kinase KIT by stem cell factor, Cell 130 (2007) 323–334.
[50] X. Shi, L.P. Sousa, E.M. Mandel-Bausch, F. Tome, A.V. Reshetnyak, Y. Hadari, et al., Distinct cellular properties of oncogenic KIT receptor tyrosine kinase mutants enable alternative courses of cancer cell inhibition, Proc. Natl. Acad. Sci. U. S. A. 113 (2016) E4784–E4793.
[51] J. Zhou, J.A. Adams, Participation of ADP dissociation in the rate-determining step in cAMP-dependent protein kinase, Biochemistry 36 (1997) 15733–15738.
[52] J. Lennartsson, P. Blume-Jensen, M. Hermanson, E. Pontén, M. Carlberg, L. Rönnstrand, Phosphorylation of Shc by Src family kinases is necessary for stem cell factor receptor/c-kit mediated activation of the Ras/MAP kinase pathway and c-fos induction, Oncogene 18 (1999) 5546–5553.
[53] S.M. Stanford, N. Bottini, Targeting tyrosine phosphatases: time to end the stigma, Trends Pharmacol. Sci. 38 (2017) 524–540.
[54] R. Roskoski Jr., Src protein-tyrosine kinase structure and regulation, Biochem. Biophys. Res. Commun. 324 (2004) 1155–1164.
[55] R. Roskoski Jr., Src kinase regulation by phosphorylation and dephosphorylation, Biochem. Biophys. Res. Commun. 331 (2005) 1–14.
[56] M.C. Frame, R. Roskoski Jr., Src family tyrosine kinases, Reference Module in Life Sciences, Elsevier, Amsterdam, 2017, pp. 1–11, http://dx.doi.org/10.1016/B978-0-12-809633-8.07199-5.
[57] H. Joensuu, P. Hohenberger, C.L. Corless, Gastrointestinal stromal tumor, Lancet 382 (2013) 973–983.
[58] A.P. Kornev, N.M. Haste, S.S. Taylor, Ten Eyck LF: Surface comparison of active and inactive protein kinases identifies a conserved activation mechanism, Proc. Natl. Acad. Sci. U. S. A. 103 (2006) 17783–17788.
[59] A.P. Kornev, S.S. Taylor, L.F. Ten Eyck, A helix scaffold for the assembly of active protein kinases, Proc. Natl. Acad. Sci. U. S. A. 105 (2008) 14377–14382.
[60] R. Roskoski Jr., Anaplastic lymphoma kinase (ALK): structure, oncogenic activation, and pharmacological inhibition, Pharmacol. Res. 68 (2013) 68–94.
[61] R. Roskoski Jr., Anaplastic lymphoma kinase (ALK) inhibitors in the treatment of ALK-driven lung cancers, Pharmacol. Res. 117 (2017) 343–356.
[62] R. Roskoski Jr., Cyclin-dependent protein kinase inhibitors including palbociclib as anticancer drugs, Pharmacol. Res. 111 (2016) 784–803.
[63] R. Roskoski Jr., ErbB/HER protein-tyrosine kinases: structures and small molecule inhibitors, Pharmacol. Res. 79 (2014) 34–74.
[64] R. Roskoski Jr., ERK1/2 MAP kinases: structure, function, and regulation, Pharmacol. Res. 66 (2012) 105–143.
[65] R. Roskoski Jr., Janus kinase (JAK) inhibitors in the treatment of inflammatory and neoplastic diseases, Pharmacol. Res. 111 (2016) 784–803.
[66] R. Roskoski Jr., Allosteric MEK1/2 inhibitors including cobimetanib and trametinib in the treatment of cutaneous melanomas, Pharmacol. Res. 117 (2017) 20–31.
[67] R. Roskoski Jr., A. Sadeghi-Nejad, Role of RET protein-tyrosine kinase inhibitors in the treatment RET-driven thyroid and lung cancers, Pharmacol. Res. 128 (2018) 1–17.
[68] R. Roskoski Jr., ROS1 protein-tyrosine kinase inhibitors in the treatment of ROS1 fusion protein-driven non-small cell lung cancers, Pharmacol. Res. 121 (2017) 202–212.
[69] R. Roskoski Jr., Vascular endothelial growth factor (VEGF) and VEGF receptor inhibitors in the treatment of renal cell carcinomas, Pharmacol. Res. 120 (2017) 116–132.
[70] H.S. Meharena, P. Chang, M.M. Keshwani, K. Oruganty, A.K. Nene, N. Kannan, et al., Deciphering the structural basis of eukaryotic protein kinase regulation, PLoS Biol. 11 (2013) e1001690.
[71] R. Roskoski Jr., Classification of small molecule protein kinase inhibitors based upon the structures of their drug-enzyme complexes, Pharmacol. Res. 103 (2016) 26–48.
[72] K. Shah, Y. Liu, C. Deirmengian, K.M. Shokat, Engineering unnatural nucleotide specificity for Rous sarcoma virus tyrosine kinase to uniquely label its direct substrates, Proc. Natl. Acad. Sci. U. S. A. 94 (1997) 3565–3570.
[73] Y. Liu, K. Shah, F. Yang, L. Witucki, K.M. Shokat, A molecular gate which controls unnatural ATP analogue recognition by the tyrosine kinase v-Src, Bioorg. Med. Chem. 6 (1998) 1219–1226.
[74] J.J. Liao, Molecular recognition of protein kinase binding pockets for design of potent and selective kinase inhibitors, J. Med. Chem. 50 (2007) 409–424.
[75] C.D. Mol, K.B. Lim, V. Sridhar, H. Zou, E.Y. Chien, B.C. Sang, et al., Structure of a c-kit product complex reveals the basis for kinase transactivation, J. Biol. Chem. 278 (2003) 31461–31464.
[76] C.D. Mol, D.R. Dougan, T.R. Schneider, R.J. Skene, M.L. Kraus, D.N. Scheibe, et al., Structural basis for the autoinhibition and STI-571 inhibition of c-Kit tyrosine kinase, J. Biol. Chem. 279 (2004) 31655–31663.
[77] K.S. Gajiwala, J.C. Wu, J. Christensen, G.D. Deshmukh, W. Diehl, J.P. DiNitto, et al., KIT kinase mutants show unique mechanisms of drug resistance to imatinib and sunitinib in gastrointestinal stromal tumor patients, Proc. Natl. Acad. Sci. U. S. A. 106 (2009) 1542–1547.
[78] A.P. Garner, J.M. Gozgit, R. Anjum, S. Vodala, A. Schrock, T. Zhou, et al., Ponatinib inhibits polyclonal drug-resistant KIT oncoproteins and shows therapeutic potential in heavily pretreated gastrointestinal stromal tumor (GIST) patients, Clin. Cancer Res. 20 (2014) 5745–5755.
[79] M. Kissova, G. Maga, E. Crespan, The human tyrosine kinase Kit and its gatekeeper mutant T670I, show different kinetic properties: implications for drug design, Bioorg. Med. Chem. 24 (2016) 4555–4562.
[80] A.C. Dar, K.M. Shokat, The evolution of protein kinase inhibitors from antagonists to agonists of cellular signaling, Annu. Rev. Biochem 80 (2011) 769–795.
[81] J. Monod, J.P. Changeux, F. Jacob, Allosteric proteins and cellular control systems, J. Mol. Biol. 6 (1963) 306–329.
[82] F. Zuccotto, E. Ardini, E. Casale, M. Angiolini, Through the gatekeeper door: exploiting the active kinase conformation, J. Med. Chem. 53 (2010) 2691–2694.
[83] L.K. Gavrin, E. Saiah, Approaches to discover non-ATP site inhibitors, Med. Chem. Commun. 4 (2013) 41.
[84] V. Lamba, I. Ghosh, New directions in targeting protein kinases: focusing upon true allosteric and bivalent inhibitors, Curr. Pharm. Des. 18 (2012) 2936–2945.
[85] F.E. Kwarcinski, K.R. Brandvold, S. Phadke, O.M. Beleh, T.K. Johnson, J.L. Meagher, et al., Conformation-selective analogues of dasatinib reveal insight into kinase inhibitor binding and selectivity, ACS Chem. Biol. 11 (2016) 1296–1304.
[86] D. Bajusz, G.G. Ferenczy, G.M. Keserá, Structure-based virtual screening approaches in kinase-directed drug discovery, Curr. Top. Med. Chem. 17 (2017) 2235–2259.
[87] D. Fabbro, S.W. Cowan-Jacob, H. Moebitz, Ten things you should know about protein kinases: IUPHAR Review 14, Br. J. Pharmacol. 172 (2015) 2675–2700.
[88] O.P. van Linden, A.J. Kooistra, R. Leurs, I.J. de Esch, C. de Graaf, KLIFS: a knowledge-based structural database to navigate kinase-ligand interaction space, J. Med. Chem. 57 (2014) 249–277.
[89] M.J. Frost, P.T. Ferrao, T.P. Hughes, L.K. Ashman, Juxtamembrane mutant V560G Kit is more sensitive to imatinib (STI571) compared with wild-type c-kit whereas the kinase domain mutant D816V Kit is resistant, Mol. Cancer Ther. 1 (2002) 1115–1124.
[90] E. Buchdunger, J. Zimmermann, H. Mett, T. Meyer, M. Müller, B.J. Druker, et al., Inhibition of the Abl protein-tyrosine kinase *in vitro* and *in vivo* by a 2-phenylaminopyrimidine derivative, Cancer Res. 56 (1996) 100–104.
[91] R. Roskoski Jr., STI-571: an anticancer protein-tyrosine kinase inhibitor, Biochem. Biophys. Res. Commun. 309 (2003) 709–717.
[92] T.A. Carter, L.M. Wodicka, N.P. Shah, A.M. Velasco, M.A. Fabian, D.K. Treiber, et al., Inhibition of drug-resistant mutants of ABL, KIT, and EGF receptor kinases, Proc. Natl. Acad. Sci. U. S. A. 102 (2005) 11011–11016.
[93] R. Roskoski Jr., Sunitinib: a VEGF and PDGF receptor protein kinase and angiogenesis inhibitor, Biochem. Biophys. Res. Commun. 356 (2007) 323–328.
[94] M.C. Heinrich, R.G. Maki, C.L. Corless, C.R. Antonescu, A. Harlow, D. Griffith, et al., Primary and secondary kinase genotypes correlate with the biological and clinical activity of sunitinib in imatinib-resistant gastrointestinal stromal tumor, J. Clin. Oncol. 26 (2008) 5352–5359.
[95] W.S. Huang, C.A. Metcalf, R. Sundaramoorthi, Y. Wang, D. Zou, R.M. Thomas, et al., Discovery of 3-[2-(imidazo[1,2-b]pyridazin-3-yl)ethynyl]-4-methyl-N-{4-[(4-methylpiperazin-1-yl)methyl]-3-(trifluoromethyl)phenyl}benzamide (AP24534), a potent, orally active pan-inhibitor of breakpoint cluster region-abelson (BCR-ABL) kinase including the T315I gatekeeper mutant, J. Med. Chem. 53 (2010) 4701–4719.
[96] D.D. Hu-Lowe, H.Y. Zou, M.L. Grazzini, M.E. Hallin, G.R. Wickman, K. Amundson, et al., Nonclinical antiangiogenesis and antitumor activities of axitinib (AG-013736), an oral, potent, and selective inhibitor of vascular endothelial growth factor receptor tyrosine kinases 1, 2, 3, Clin. Cancer Res. 14 (2008) 7272–7283.
[97] A. Bellesoeur, E. Carton, J. Alexandre, F. Goldwasser, O. Huillard, Axitinib in the treatment of renal cell carcinoma: design, development, and place in therapy, Drug Des. Dev. Ther. 11 (2017) 2801–2811.
[98] W. Sherman, T. Day, M.P. Jacobson, R.A. Friesner, R. Farid, Novel procedure for modeling ligand/receptor induced fit effects, J. Med. Chem. 49 (2006) 534–553.
[99] R.A. Friesner, J.L. Banks, R.B. Murphy, T.A. Halgren, J.J. Klicic, D.T. Mainz, et al., Glide: a new approach for rapid, accurate docking and scoring: 1 Method and assessment of docking accuracy, J. Med. Chem. 47 (2004) 1739–1749.
[100] F.M. Yakes, J. Chen, J. Tan, K. Yamaguchi, Y. Shi, P. Yu, et al., Cabozantinib (XL184), a novel MET and VEGFR2 inhibitor, simultaneously suppresses metastasis, angiogenesis, and tumor growth, Mol. Cancer Ther. 10 (2011) 2298–2308.
[101] J.N. Markowitz, K.M. Fancher, Cabozantinib: a multitargeted oral tyrosine kinase inhibitor, Pharmacotherapy 38 (2018) 357–369.
[102] M.M. Schittenhelm, S. Shiraga, A. Schroeder, A.S. Corbin, D. Griffith, F.Y. Lee, et al., Dasatinib (BMS-354825), a dual SRC/ABL kinase inhibitor, inhibits the kinase activity of wild-type, juxtamembrane, and activation loop mutant KIT isoforms associated with human malignancies, Cancer Res. 66 (2006) 473–481.
[103] N.P. Shah, F.Y. Lee, R. Luo, Y. Jiang, M. Donker, C. Akin, Dasatinib (BMS-354825) inhibits KIT D816V, an imatinib-resistant activating mutation that triggers

neoplastic growth in most patients with systemic mastocytosis, Blood 108 (2006) 286–291.
[104] L.J. Lombardo, F.Y. Lee, P. Chen, D. Norris, J.C. Barrish, K. Behnia, et al., Discovery of *N*-(2-chloro-6-methyl- phenyl)-2-(6-(4-(2-hydroxyethyl)- piperazin-1-yl)-2-methylpyrimidin-4- ylamino)thiazole-5-carboxamide (BMS-354825), a dual Src/Abl kinase inhibitor with potent antitumor activity in preclinical assays, J. Med. Chem. 47 (2004) 6658–6661.
[105] Z. Chen, F.Y. Lee, K.N. Bhalla, J. Wu, Potent inhibition of platelet-derived growth factor-induced responses in vascular smooth muscle cells by BMS-354825 (dasatinib), Mol. Pharmacol. 69 (2006) 1527–1533.
[106] P.C. Amrein, The potential for dasatinib in treating chronic lymphocytic leukemia, acute myeloid leukemia, and myeloproliferative neoplasms, Leuk. Lymphoma 52 (2011) 754–763.
[107] C.R. Antonescu, K.J. Busam, T.D. Francone, G.C. Wong, T. Guo, N.P. Agaram, et al., L576P KIT mutation in anal melanomas correlates with KIT protein expression and is sensitive to specific kinase inhibition, Int. J. Cancer 121 (2007) 257–264.
[108] K.L. Ashman, R. Griffith, Therapeutic targeting of c-KIT in cancer, Expert Opin. Investig. Drugs 22 (2013) 103–115.
[109] J. Matsui, Y. Yamamoto, Y. Funahashi, A. Tsuruoka, T. Watanabe, T. Wakabayashi, et al., E7080, a novel inhibitor that targets multiple kinases, has potent antitumor activities against stem cell factor producing human small cell lung cancer H146, based on angiogenesis inhibition, Int. J. Cancer 122 (2008) 664–671.
[110] S.M. Wilhelm, J. Dumas, L. Adnane, M. Lynch, C.A. Carter, G. Schütz, et al., Regorafenib (BAY 73–4506): a new oral multikinase inhibitor of angiogenic, stromal and oncogenic receptor tyrosine kinases with potent preclinical antitumor activity, Int. J. Cancer 129 (2011) 245–255.
[111] S. Wilhelm, D.S. Chien, BAY 43–9006: preclinical data, Curr. Pharm. Des. 8 (2002) 2255–2257.
[112] D. Strumberg, Preclinical and clinical development of the oral multikinase inhibitor sorafenib in cancer treatment, Drugs Today (Barc.) 41 (2005) 773–784.
[113] T. Guo, N.P. Agaram, G.C. Wong, G. Hom, D. D'Adamo, R.G. Maki, et al., Sorafenib inhibits the imatinib-resistant KIT^{T670I}gatekeeper mutation in gastrointestinal stromal tumor, Clin. Cancer Res. 13 (2007) 4874–4881.
[114] D.J. DeAngelo, T.I. George, A. Linder, C. Langford, C. Perkins, J. Ma, et al., Efficacy and safety of midostaurin in patients with advanced systemic mastocytosis: 10-year median follow-up of a phase II trial, Leukemia 32 (2018) 470–478.
[115] R.M. Stone, P.W. Manley, R.A. Larson, R. Capdeville, Midostaurin: its odyssey from discovery to approval for treating acute myeloid leukemia and advanced systemic mastocytosis, Blood Adv. 2 (2018) 444–453.
[116] J.D. Growney, J.J. Clark, J. Adelsperger, R. Stone, D. Fabbro, J.D. Griffin, et al., Activation mutations of human c-KIT resistant to imatinib mesylate are sensitive to the tyrosine kinase inhibitor PKC412, Blood 106 (2005) 721–724.
[117] S. Atwell, J.M. Adams, J. Badger, M.D. Buchanan, I.K. Feil, K.J. Froning, et al., A novel mode of Gleevec binding is revealed by the structure of spleen tyrosine kinase, J. Biol. Chem. 279 (2004) 55827–55832.
[118] R.M. Touyz, N.N. Lang, J. Herrmann, A.H. van den Meiracker, A.H.J. Danser, Recent advances in hypertension and cardiovascular toxicities with vascular endothelial growth factor inhibition, Hypertension 70 (2017) 220–226.
[119] M. Savi, C. Frati, S. Cavalli, G. Graiani, S. Galati, A. Buschini, et al., Imatinib mesylate-induced cardiomyopathy involves resident cardiac progenitors, Pharmacol. Res. 127 (2018) 15–25.
[120] N.A. Gude, M.A. Sussman, Chasing c-Kit through the heart: taking a broader view, Pharmacol. Res. 127 (2018) 110–115.
[121] F. Carles, S. Bourg, C. Meyer, P. Bonnet, PKIDB: a curated, annotated and updated database of protein kinase inhibitors in clinical trials, Molecules 23 (2018), http://dx.doi.org/10.3390/molecules23040908.
[122] B.L. Roth, D.J. Sheffler, W.K. Kroeze, Magic shotguns versus magic bullets: selectively non-selective drugs for mood disorders and schizophrenia, Nat. Rev. Drug Discov. 3 (2004) 353–359.
[123] R. Roskoski Jr., Guidelines for preparing color figures for everyone including the colorblind, Pharmacol. Res. 119 (2017) 240–241.